Biopotential Sensing and Analog Signal Processing for Health Monitoring and Brain Interfaces

Gert Cauwenberghs
University of California San Diego
gert@ucsd.edu

Biopotential Sources and Signals

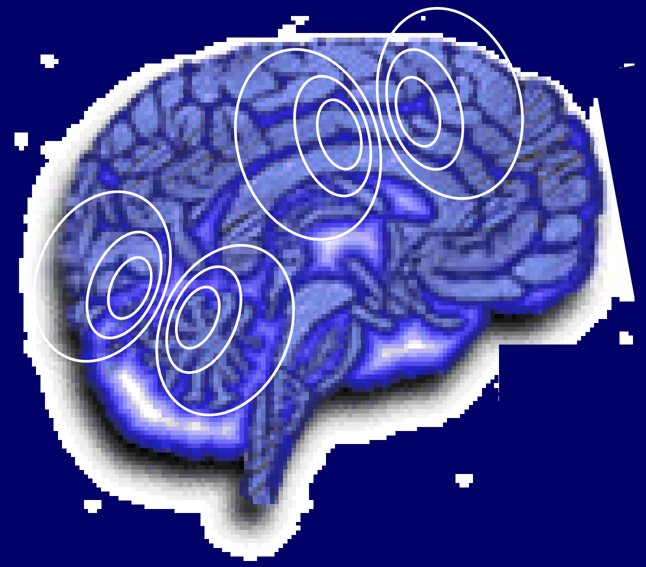

Action Potentials

Local Fields

Body Surface Biopotentials

Generation and Propagation of Biopotentials

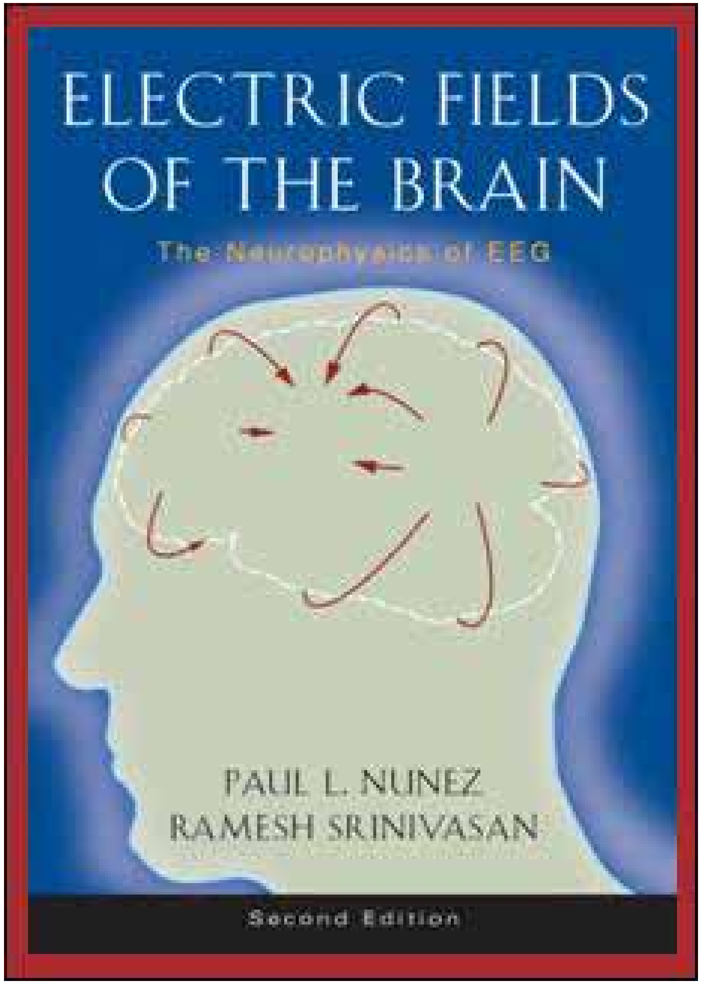

Paul L. Nunez and Ramesh Srinivasan, *Electric Fields of the Brain—The Neurophysics of EEG*, 2nd Ed., Oxford University Press, 2006.

Neuron Action Potentials and Synaptic Currents

- Neurons transmit information by electrical signals (**action potentials**, or **spikes**).
- At insulating gaps (**synapses**), presynaptic neurons release **neurotransmitters** upon each action potential.
- The postsynaptic neuron receives and integrates the neurochemical current.
- Downstream changes decide whether the incoming activity will be **propagated** or **suppressed**.
- Diffusible **neuromodulators** (such NO) further regulate neural function through long-range chemical transport, and local receptor binding at the neuron membrane.

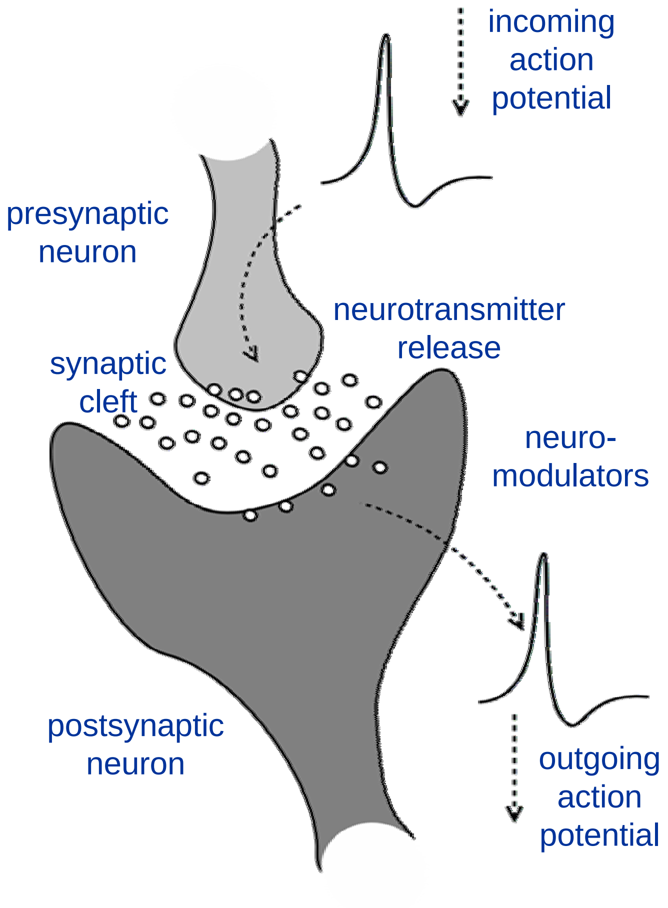

Synaptic Currents and Volume Conduction

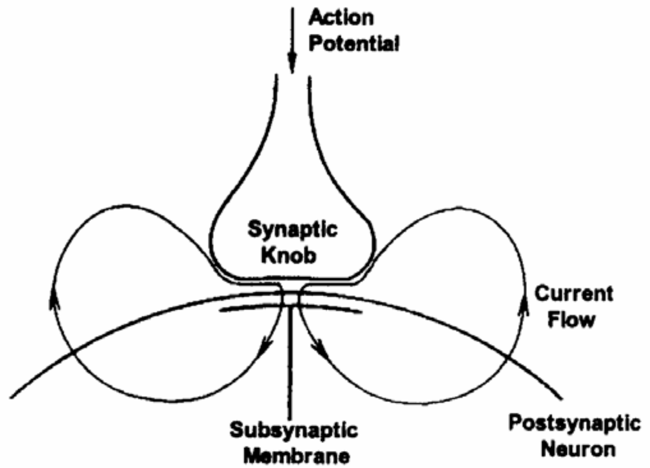

Figure 4-6 Membrane current due to local excitatory synaptic action. An action potential propagating along the presynaptic axon activates a neurotransmitter in the synaptic knob that changes local membrane conductivities to select ions, thereby producing a local current sink and more distant distributed sources to preserve current conservation.

Table 4-1 Typical resistivity of several materials and tissues

Material	Resistivity (Ω cm)
Copper	2×10^{-6}
Seawater	20
CSF	64
Blood	150
Spinal cord (longitudinal)	180
Cortex (5 kHz)	230
Cortex (5 Hz)	350
White matter (average)	650
Spinal cord (transverse)	1200
Bone (100 Hz)	8,000–16,000
Pure water	2×10^{7}
Active membrane (squid axon)	2×10^{7}
Passive membrane (squid axon)	10^{9}

– Postsynaptic currents triggered by action potentials (spikes) give rise to local field potentials (LFPs) through volume conduction in extracellular space.
  - *Excitatory* synapse: local current *sink*
  - *Inhibitory* synapse: local current *source*

Nunez and Srinivasan 2006, p. 153-154

Current Source/Sink Dipole Electric Field

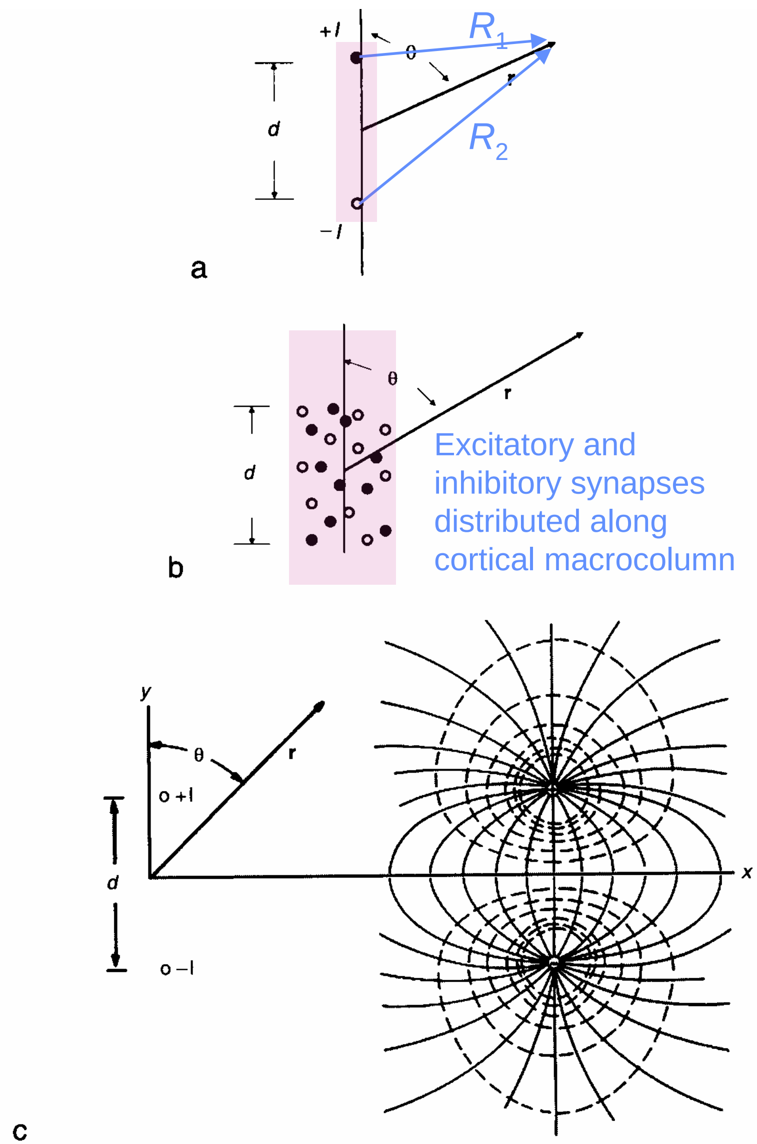

- Coherent (synchronous) activity over a distribution of synapses generates, to first order, a dipole field:

$$\Phi(\mathbf{r}) = \frac{I}{4\pi\sigma}\left(\frac{1}{R_1} - \frac{1}{R_2}\right) \cong \frac{I}{4\pi\sigma}\,\frac{d\cos\theta}{r^2}$$

- Dipoles align along macrocolumns, because of their polarization in the distribution of excitatory and inhibitory synapses.

- Synchronous dipoles add coherently; asynchronous dipoles add incoherently.

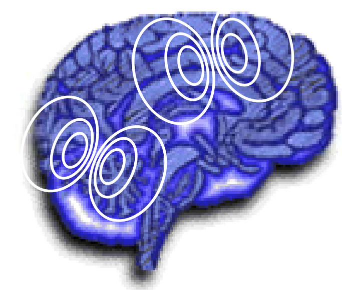

Figure 5-8 (a) The usual *current dipole* consisting of a point source $+I$ and a point sink $-I$, separated by a distance d. (b) A region of distributed sources and sinks. If local current is conserved, the potential at large distances is also dipolar, but with an effective pole separation d_{eff} smaller than d. With perfect source–sink symmetry, $d_{\text{eff}} \to 0$ and a so-called closed field is generated, as in fig. 5-5. (c) Dipole current lines (solid) and equipotentials (dashed) are plotted. These patterns occur in the saltwater tank if the tank walls and water surface are all located far from the dipole and both recording electrodes. Boundary surfaces tend to compress current lines and increase potentials.

Nunez and Srinivasan 2006, p. 215

Effect of Skull and Scalp: ECoG and EEG

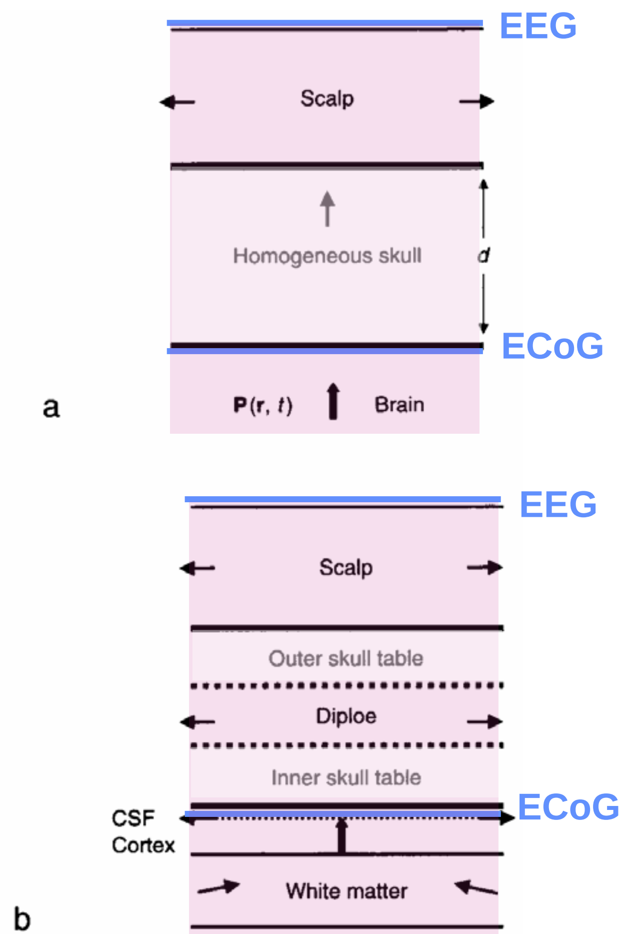

Table 4-2 Skull resistivity reported in the literature

Skull condition	Resistivity (Ω cm)	Frequency (Hz)	Reference
Dead, dry	10^{13}		Rush and Driscoll 1969
Dead, hydrated	10,000–20,000	500	Rush and Driscoll 1969
Dead, hydrated	13,000–21,000	100	Law 1993
Dead, suitures	3,500–10,000	100	Law 1993
Dead, hydrated	13,000–86,000	20	Akhatari *et* al. 2000
Live, 3 layers	4,600–21,000	20	Akhatari et al. 2000
Live	7,700	10–1000	Oostendorp et al. 2000
Dead, hydrated	6,700	$10–10^5$	Oostendorp et al. 2000
Live	1,200–3,100	10	Hoekema et al. 2003

Modified from Hoekema et al. (2003).

- Electrocorticogram (ECoG)
  - *Intracranial (invasive), on the cortical surface*
  - *Local features (cortical surface LFPs)*
  - *Epilepsy monitoring and mapping*
- Electroencephalogram (EEG)
  - *Non-invasive, on the scalp*
  - *Global features (brain waves)*
  - *Brain-computer interfaces (BCI)*

Figure 4-4 (a) A common volume conductor model of the head is the *three-sphere model*. It consists of an inner sphere (brain) and surrounded by two concentric spherical shells (skull and scalp). More complicated models may not be more accurate if tissue boundaries and (especially) tissue resistivities are not known with sufficient accuracy. (b) A more realistic geometric model consists of two additional skull layers and a layer of cerebral spinal fluid (CSF). Current shunting through the middle skull layer (diploe), CSF, and scalp is indicated by arrows. The effective skull resistivity in the *three-sphere model* (a) is larger than the actual skull resistivity in (b).

Nunez and Srinivasan 2006, p. 156-157

Neural Signals - Spikes
(Action Potentials)

- Single unit firings.
- Recorded via microelectrodes placed close to the neuron cell body.
- Amplitude as high as 500 μV and frequency content up to 7 kHz.

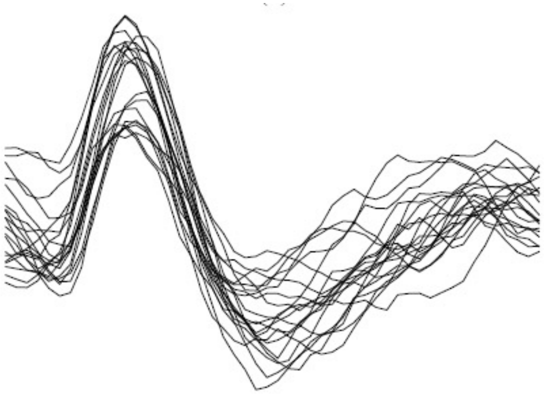

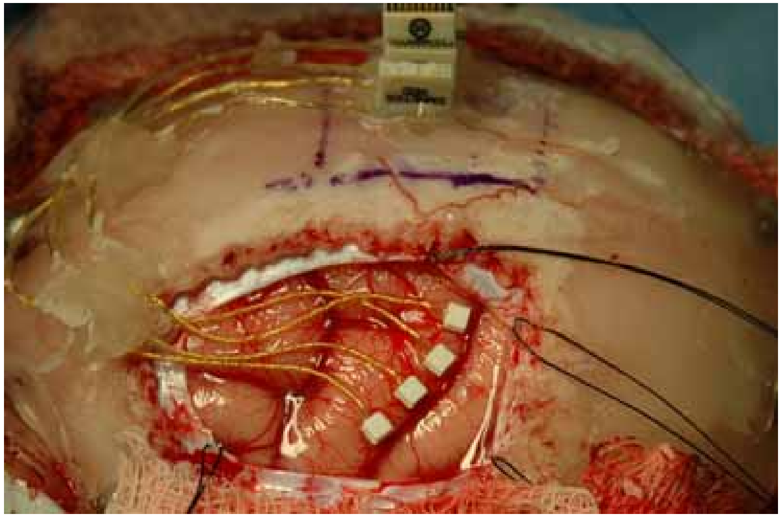

Mollazadeh et al.

Neural Signals - LFP

(Local Field Potentials)

- Summation of pre- and postsynaptic activity from a population of neurons around the electrode tip.
- Recorded via microelectrodes or lower impedance electrodes.
- Amplitude as high as 1 mV and frequency content up to 200 Hz.

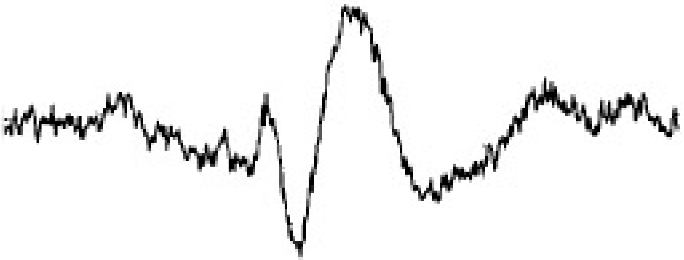

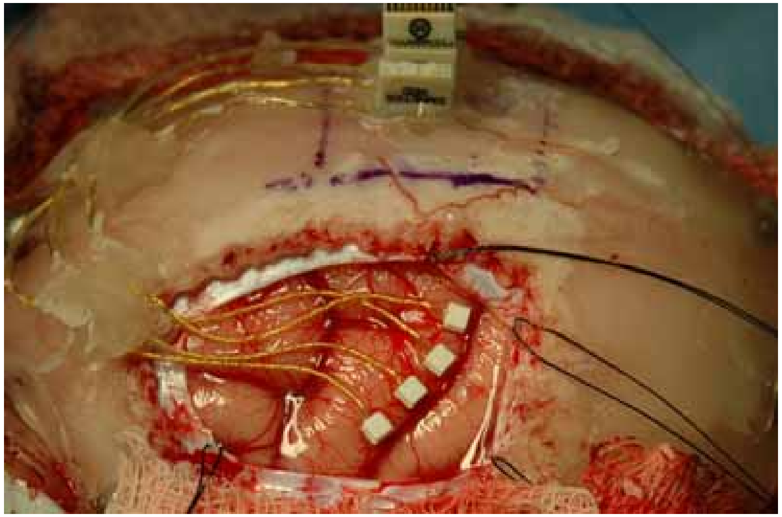

Mollazadeh et al.

Neural Signals - ECoG

(Electro-cortico-gram)

- Electrical activity on the cortical surface resulting from volume conduction of coherent collective neural activity throughout cortex.
- Recorded via surface (disk) electrodes.
- Amplitude as high as 5 mV and frequency content up to 200 Hz.

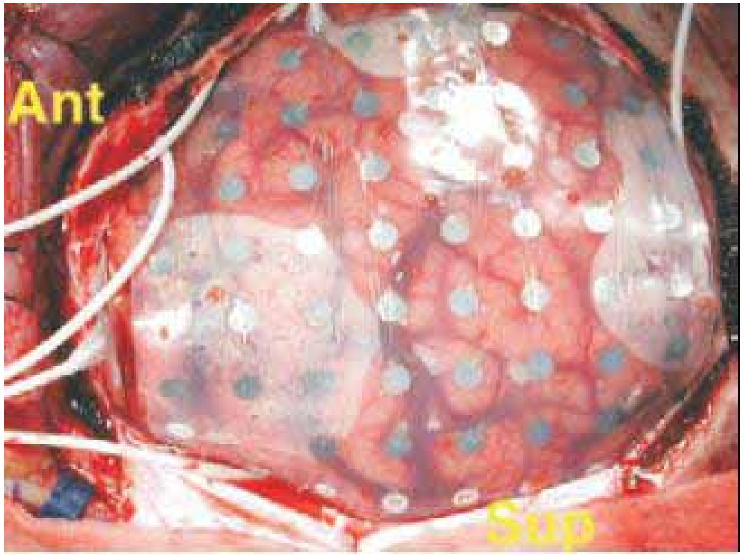

Leuthhardt et al.

Neural Signals - EEG

(Electro-encephalo-gram)

- Electrical activity on the scalp resulting from volume conduction of coherent collective neural activity through the brain and skull, and laterally along the scalp.
- Recorded via surface (disk) electrodes.
- Amplitude as high as 300 μV and frequency content up to 100 Hz.

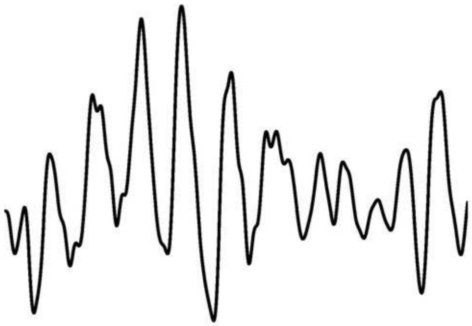

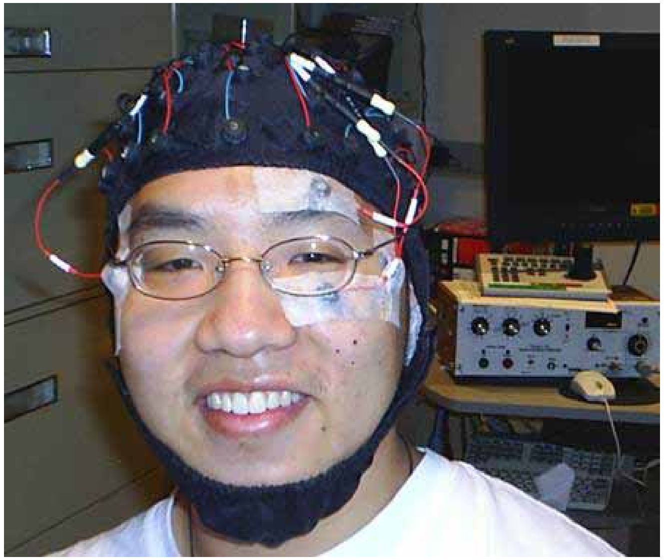

Acharya et al.

Other Biopotential Signals on Body Surface

- ***Surface electromyograms* (EMG)**
  - 10 μVpp-1mVpp, 10Hz-1kHz
  - recorded on the skin near muscles of interest
  - conveying neural activity controlling muscle contraction and particularly useful for motor prostheses
- ***Electrooculograms* (EOG)**
  - 100 μVpp-1mVpp, 10Hz-1kHz
  - recorded on the frontal skull near the eyes
  - a form of EMG conveying gaze direction useful for eye tracking in human-computer interfaces
- ***Electrocardiograms* (ECG)**
  - 10 μVpp-10mVpp, 0.1-100Hz
  - recorded on the chest
  - conveying heart activity for monitoring of health in cardiac patients and also useful in athletic fitness monitoring and detection of emotional state.

Biosignal Recording

Electrodes

Amplifiers

Signal Conditioning

Telemetry

Electrodes

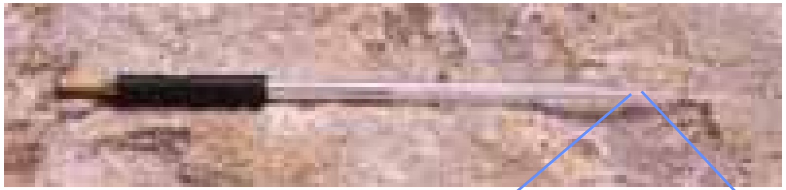

needle microelectrode
Kation Scientific

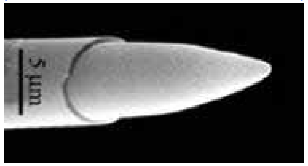

- **Needle electrode**
  - Metal, typically Tungsten
  - Electrical contact impedance in 10kΩ to 1MΩ range
  - Penetration through neural tissue

active EEG gel-contact electrode
Biosemi

- **Flat electrode**
  - Higher impedance
  - Mostly for external use and on neural surface
    - *scalp EEG (electroencephalogram) recording*
    - *retinal implants*

Electrode Arrays

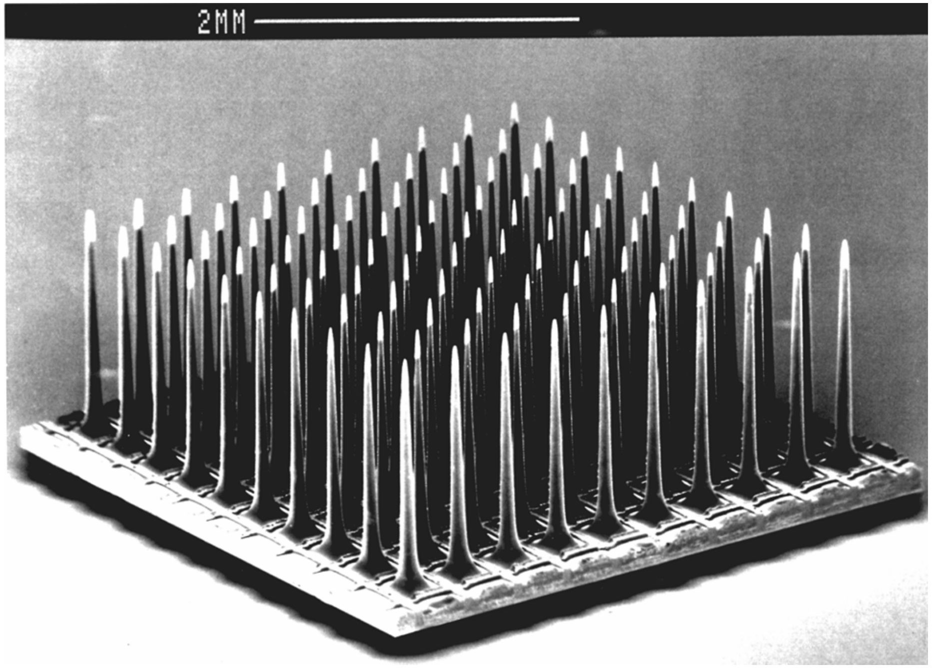

"Utah array"
Normann laboratory, University of Utah, 2003

- **Penetrating electrode arrays**
  - Typically silicon based, fabricated in MEMS (microelectromechanical systems) process
  - Cortical vision implants
- **Flat electrode arrays**
  - Retinal implants
  - Electrocorticogram (ECoG) monitoring systems

Electrocorticogram (ECoG) Recording

Implanted epilepsy grid electrodes
www.mayoclinic.com

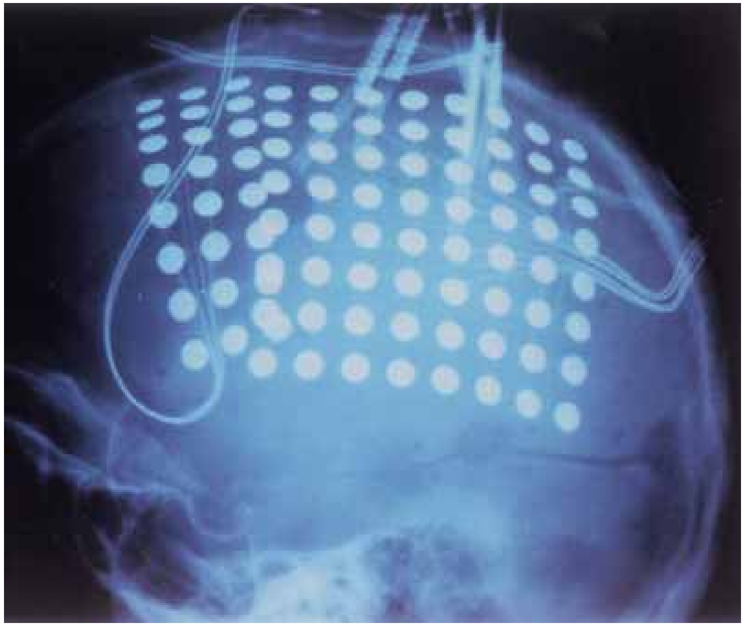

- **Cortical surface electrodes**
  - Higher spatial resolution than scalp EEG
- **Epilepsy monitoring**
  - Preparation for surgery to remove focus of epileptic activity, avoiding critical brain functional areas

Scalp EEG Recording

BioSemi Active2
www.biosemi.com

- **State of the art EEG recording**
  - 32-256 channels
  - Gel contact electrodes
  - Tethered to acquisition box
  - Off-line analysis

Gel-Based Wet-Contact EEG Electrodes

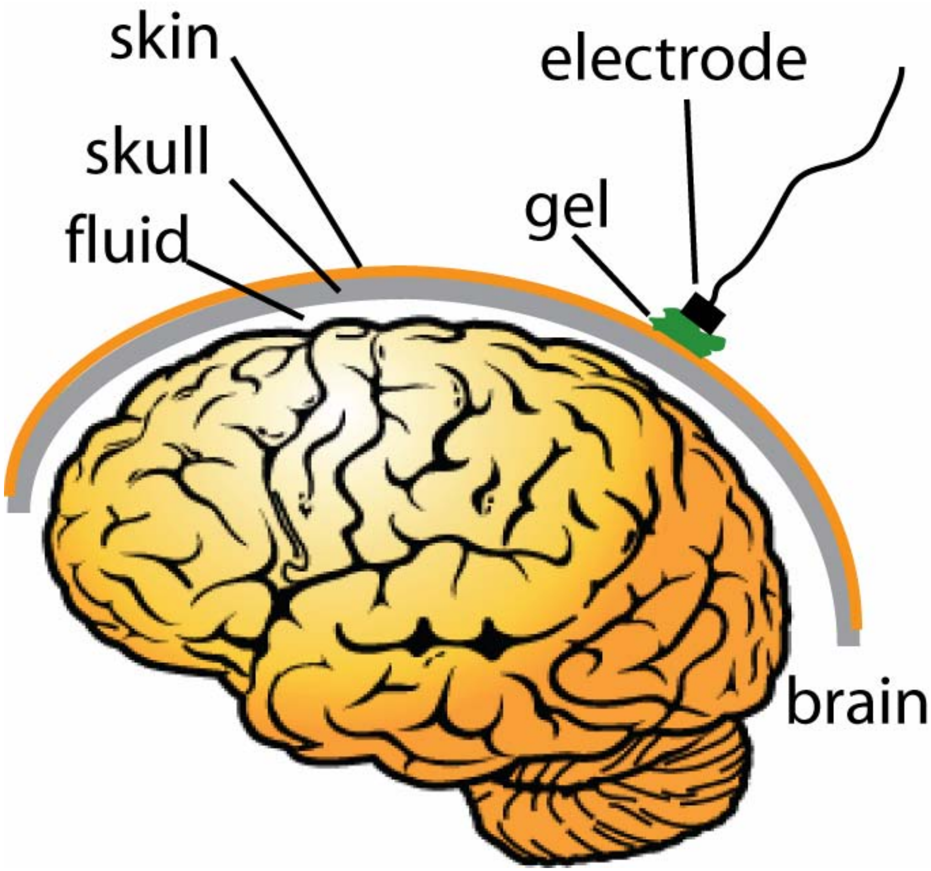

Amplitude (typ.):
1-100 μV
Bandwidth:
1-100 Hz
Impedance:
10-100kΩ

Dry-Contact EEG Electrodes

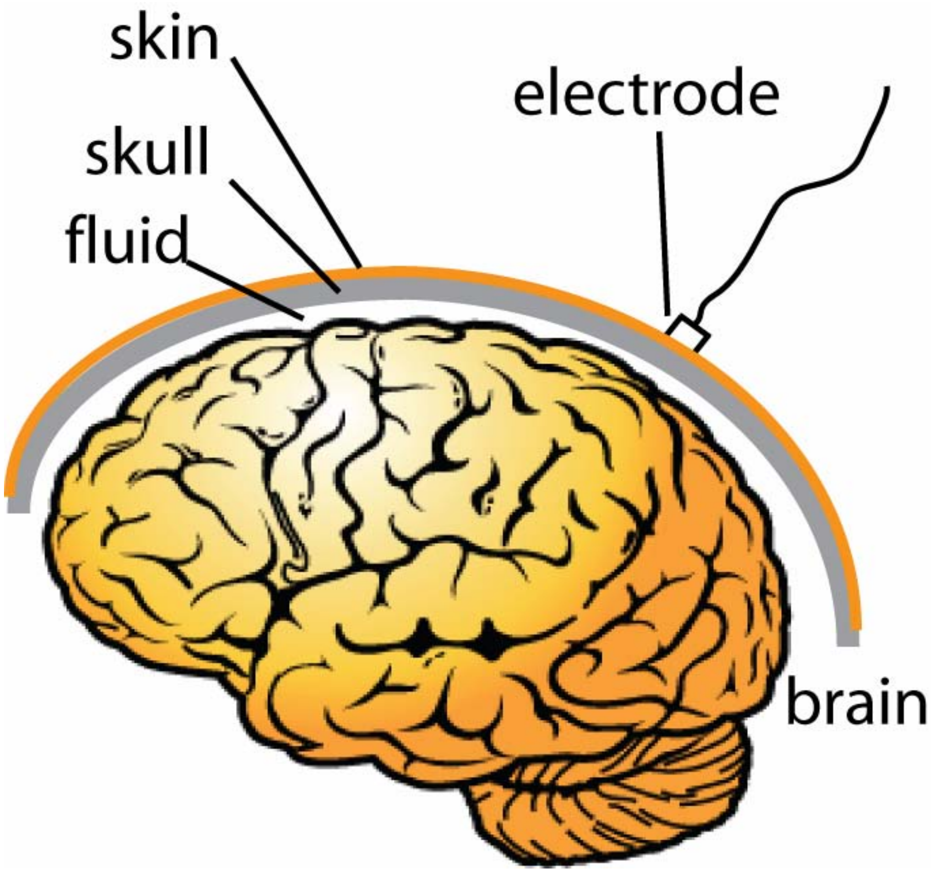

Dry-contact electrode penetrates outer layer of skin for ohmic contact without conductive gel.

Wireless EEG/ICA Neurotechnology

Sullivan, Deiss, Jung and Cauwenberghs, ISCAS'2007

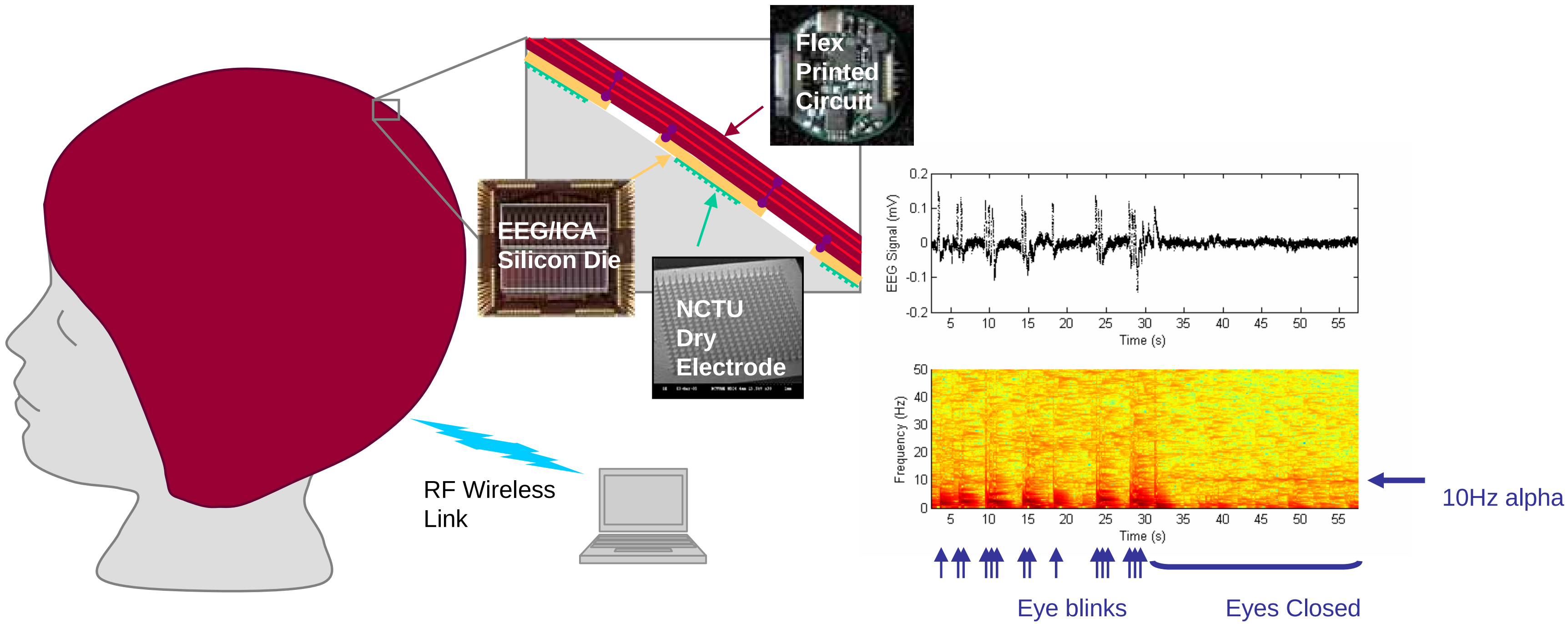

- **Integrated EEG/ICA wireless EEG recording system**
  - Scalable towards 1000+ channels
  - Dry contact electrodes (NCTU, Taiwan)
  - Wireless, lightweight
  - Extends to integrate local independent component analysis (ICA)

Non-Contact EEG Electrode

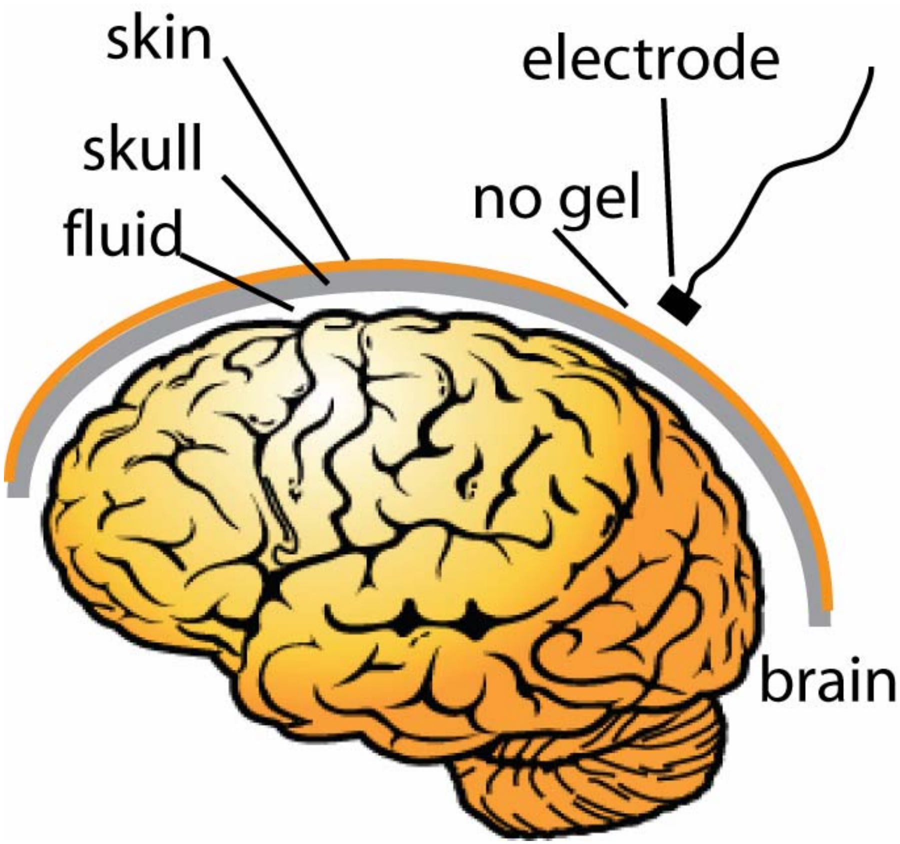

Capacitive coupling, rather than ohmic contact, between scalp/skin and electrode

Richardson & Lopez, 1970. Matsuo, et.al. 1973. And others

Capacitively-Coupled Sensor Design

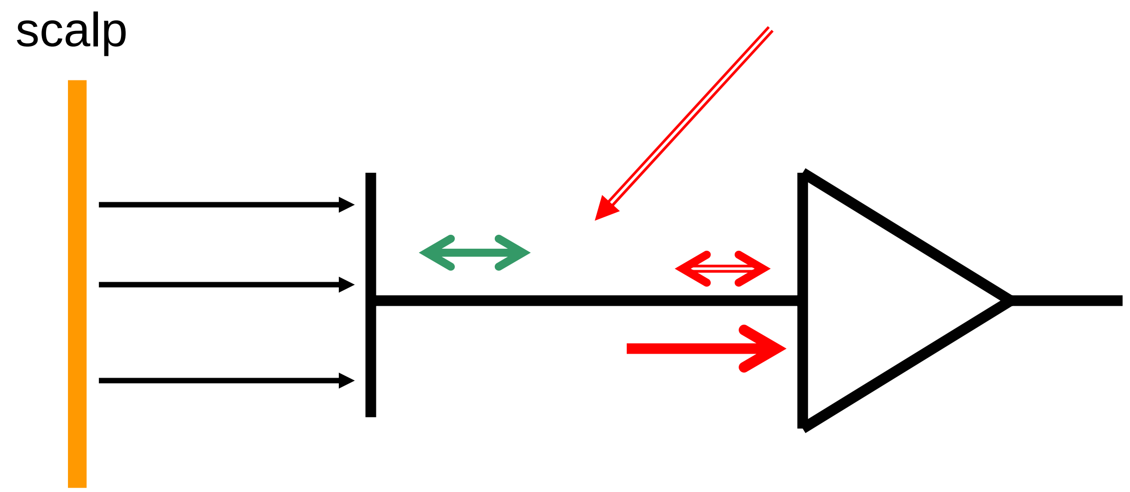

- **Design Challenges**
  - High impedance input node
    - *Current noise integrates to large input voltage noise at low frequencies*
    - *Parasitic currents (amplifier input bias current, PCB)*
    - *External noise pickup*
  - Size, Power, Cost

Capacitive Sensor and Interface Circuit

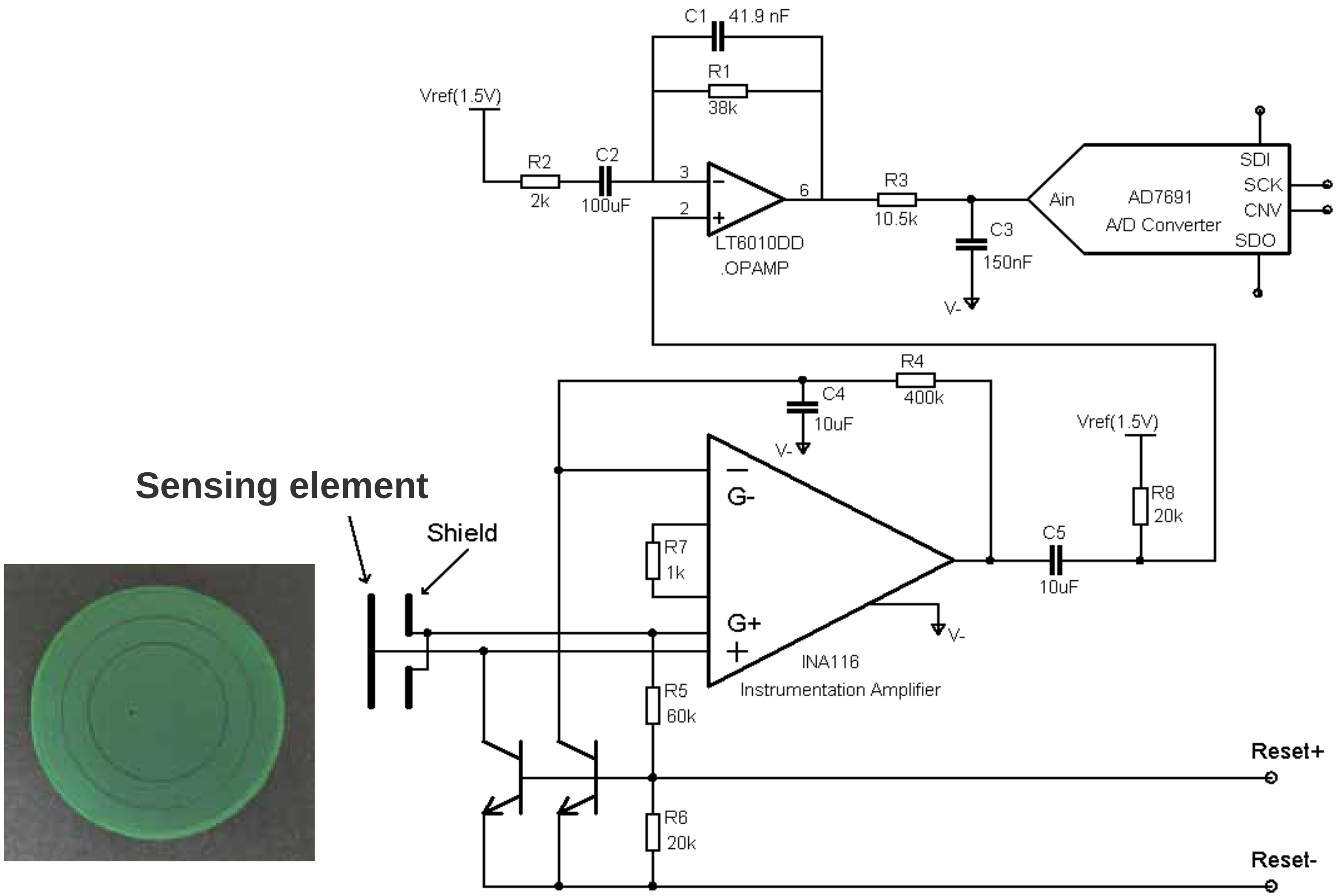

Non-Contact Sensing at Varying Distance

Gain vs. frequency

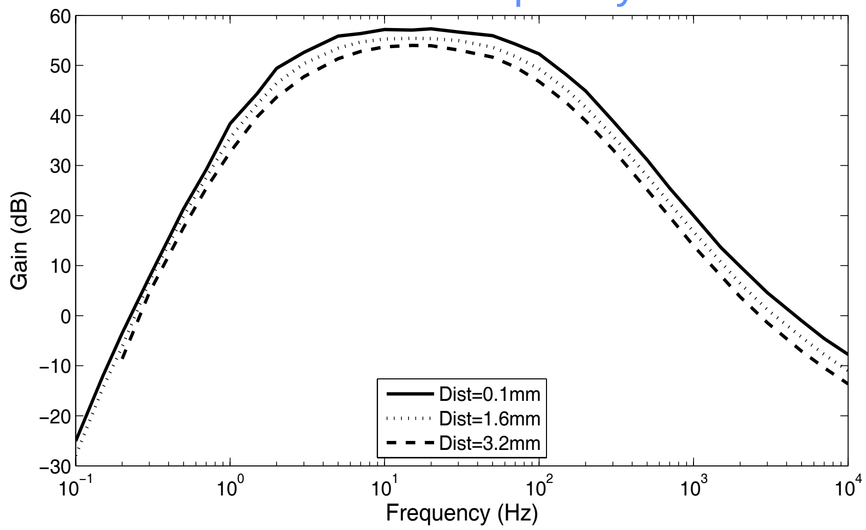

Gain vs. distance

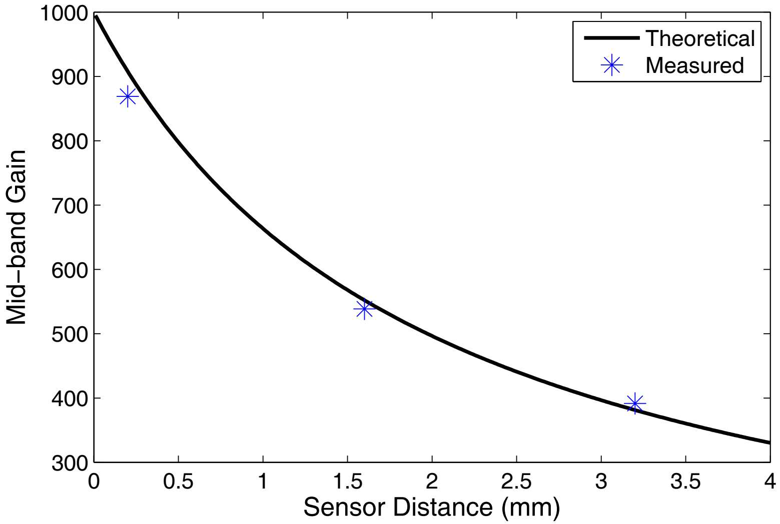

Noise vs. distance

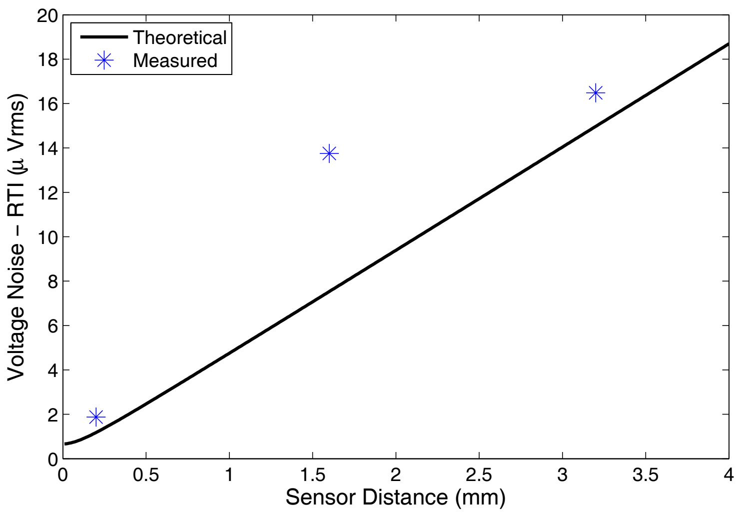

– Gain is weakly dependent on distance, owing to active shielding.
– Noise approaches low levels of wet-contact electrodes at near-zero distances.

Recorded EEG Alpha Wave Activity

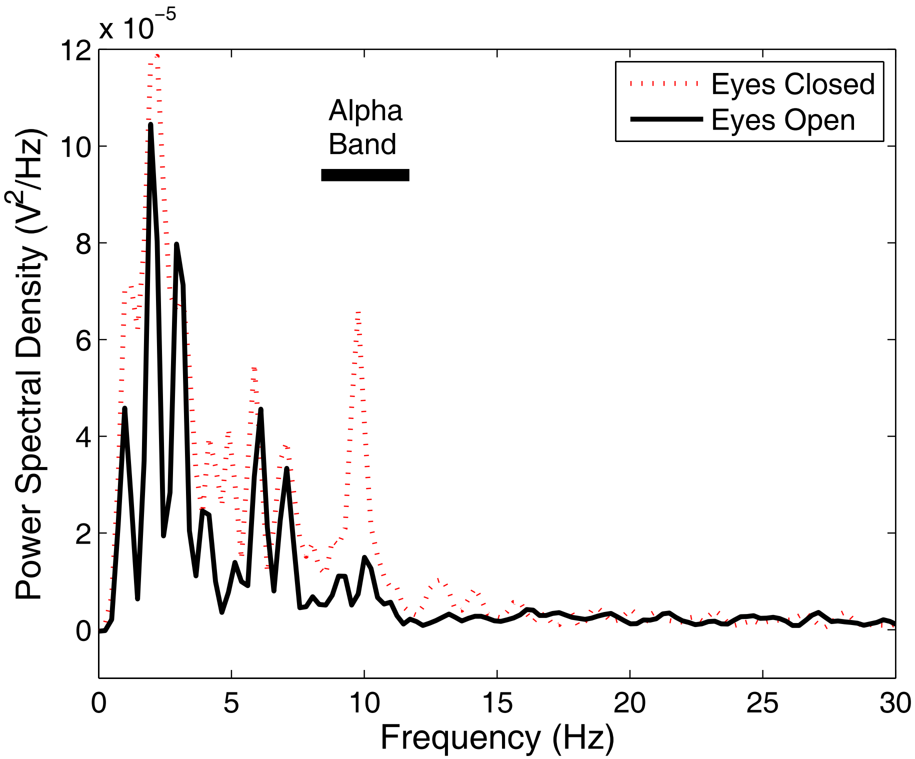

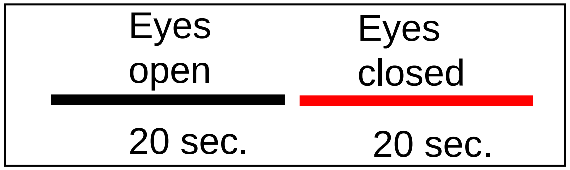

Neurosensory Engineering

“in vivo” sensing/control of neural/synaptic activity

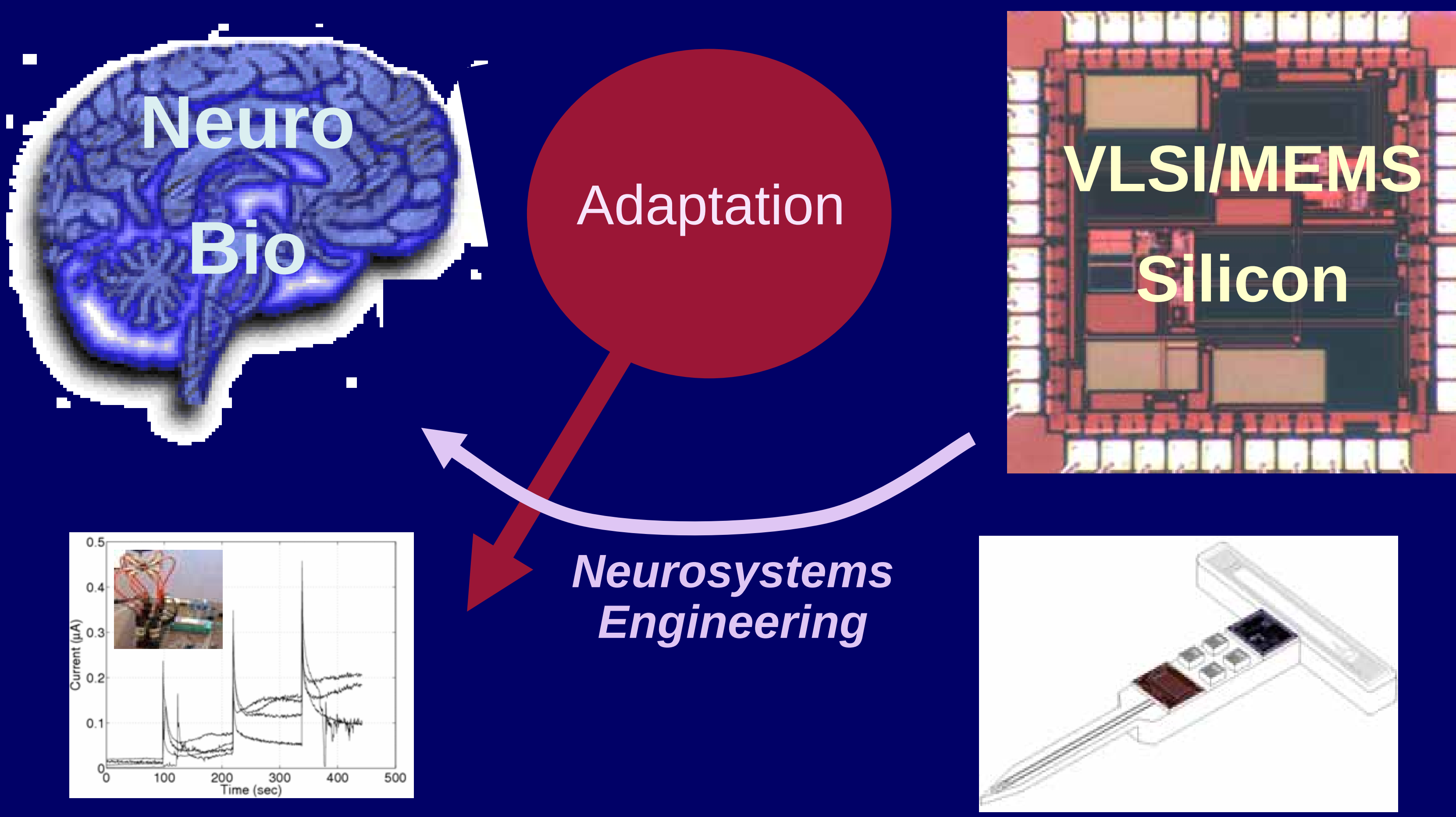

EEG/ECoG/EMG Amplification, Filtering and Quantization

Mollazadeh, Murari, Cauwenberghs and Thakor (2007)

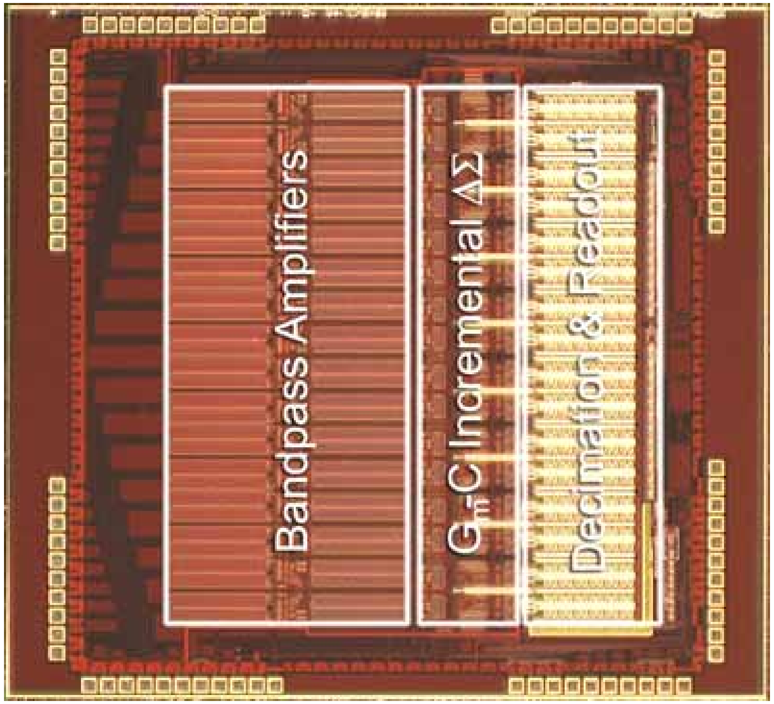

- Low noise
  - *21nV/√Hz input-referred noise*
  - *2.0μVrms over 0.2Hz-8.2kHz*
- Low power
  - *100μW per channel at 3.3V*
- Reconfigurable
  - *0.2-94Hz highpass, analog adjustable*
  - *140Hz-8.2kHz lowpass, analog adjustable*
  - *34dB-94dB gain, digitally selectable*
- High density
  - *16 channels*
  - *3.3mm X 3.3mm in 0.5μm 2P3M CMOS*
  - *0.33 sq. mm per channel*

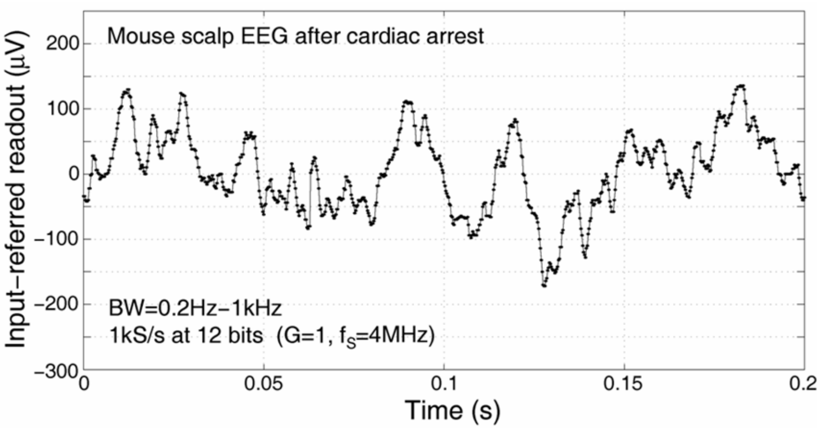

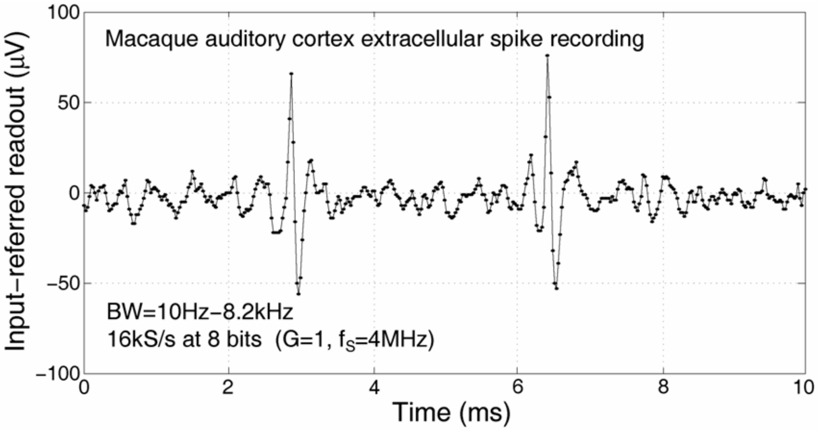

Neuropotential Interface: Circuit Design

- **VLSI system with programmable:**
  - Bandwidth to separate different modalities of neural signals
  - Midband gain (100-400)
  - ADC resolution (8-12 bits)

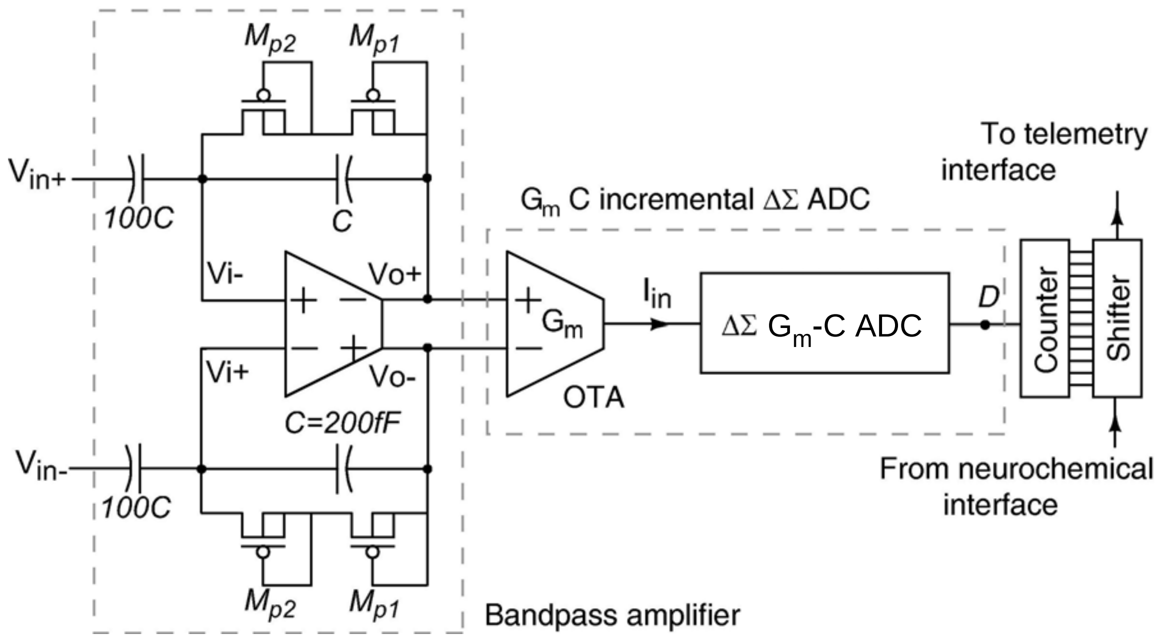

Neuropotential Interface: Circuit Design

- **Front-end amplifier**
  - Capacitive feedback bandpass topology after Harrison and Charles (2003)
  - Fully differential two stage voltage amplifier
  - Fixed midband analog gain of 40 dB
  - High frequency lowpass cutoff is selectable by amplifier bias current
  - Low frequency highpass cutoff is set by high-resistance feedback elements

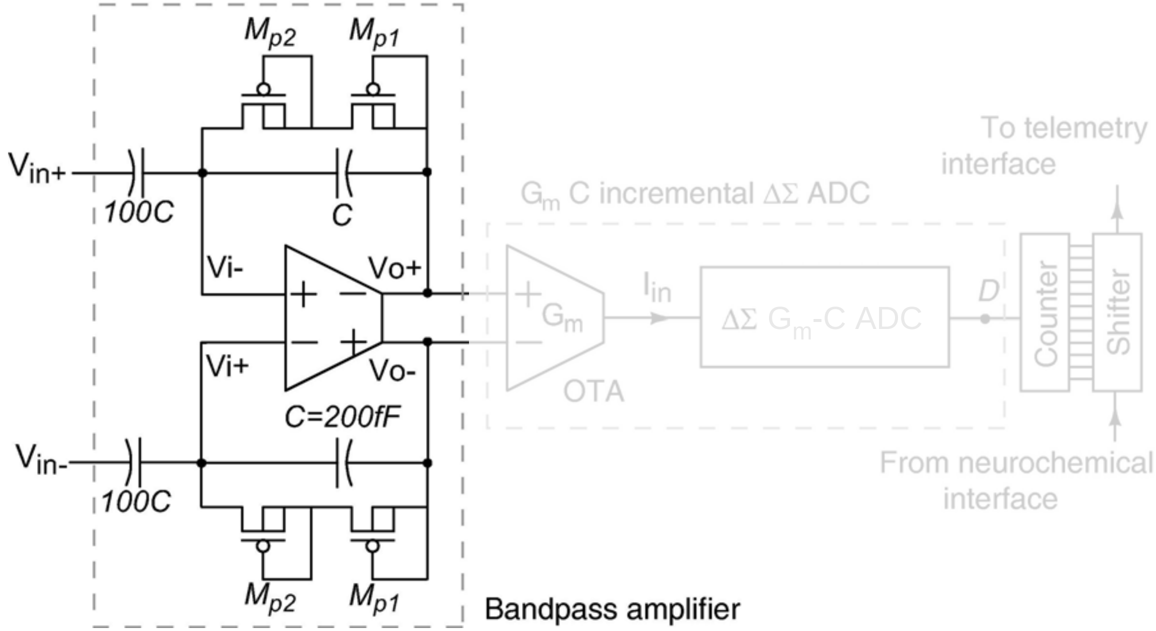

Neuropotential Interface: Results

- Measured gain: 39.7 dB
- Low frequency cutoff: 0.2 Hz
- High frequency cutoff: tunable from 0.14 – 8.2 kHz
- THD[1] < 1%
- PSRR[2] >76 dB
- CMRR[3] >82 dB

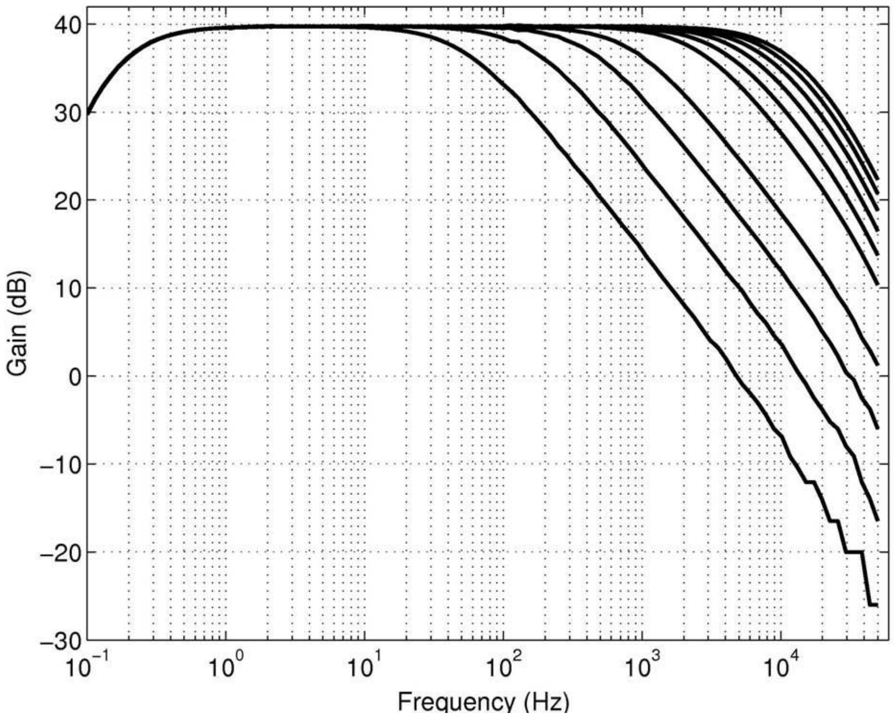

[1]THD: Total harmonic distortion

[2]PSRR: Power supply rejection ratio

[3]CMRR: Common mode rejection ratio

Neuropotential Interface: Results

- **The digitized output has:**
  - THD of less than 0.3% for input signals smaller than 1 mV
  - Noise of 1.2 LSB

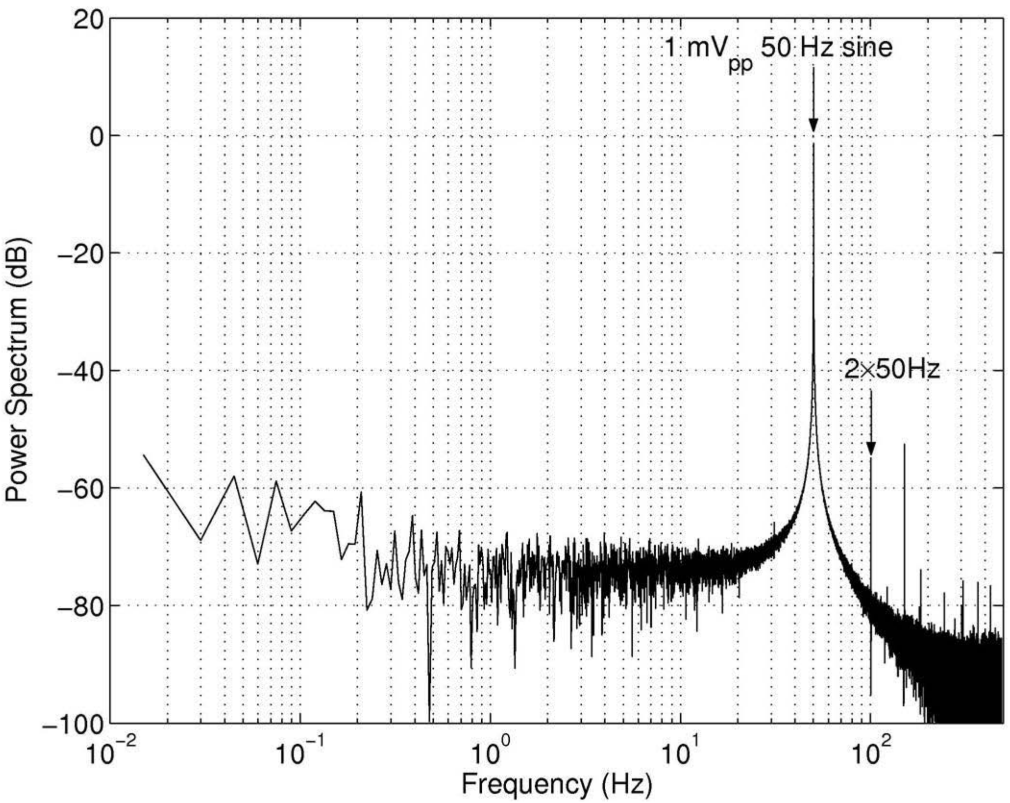

Power spectrum of the digital output of the system with a 50Hz 1 mV_{pp} sinusoidal input presented to the system.

Joint Electrical and Chemical Neural Recording

- Neuropotential and neurochemical signals are interrelated, and are implicated in several basic and clinical neural pathways.
  - *For example, the death of dopaminergic neurons is implicated in Parkinson's disease.*
- Simultaneous electrophysiological and neurochemical measurement allows to monitor these interactions or diagnose neural disease.

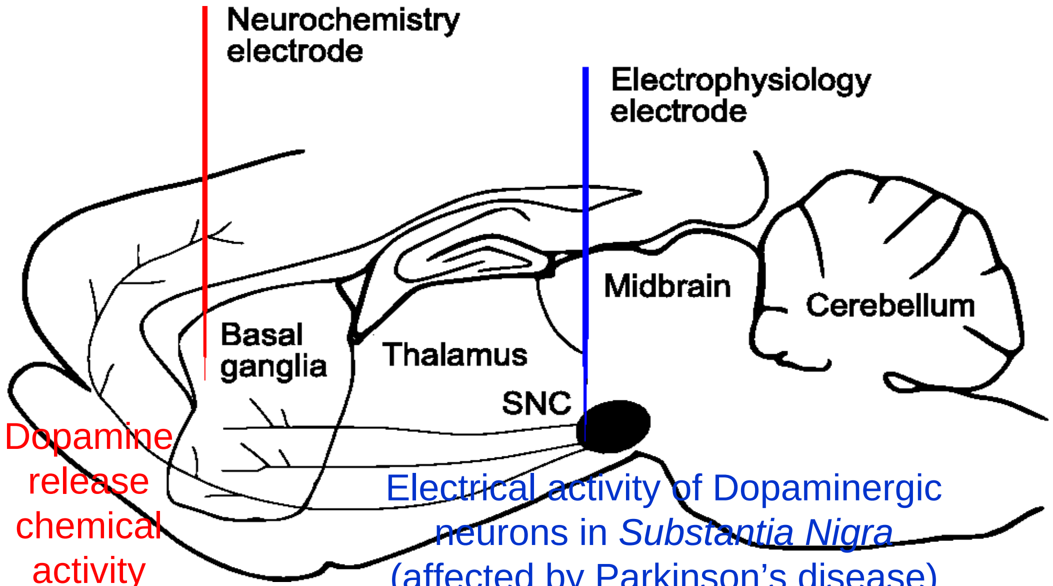

Neurotransmitter Detection

- **Neurotransmitters:**
  - Messenger molecules between neurons
    - *Dopamine, Glutamate, GABA etc.*
  - Key to understanding neural pathways
  - Neural disease etiology

- **Detection:**
  - Optical
  - Chromatography
  - Electrochemical
    - *Fast*
      - *response time < 1ms*
    - *Sensitive*
      - *1nA ≡ 10fM*
    - *System integration*
      - *in vivo monitoring*

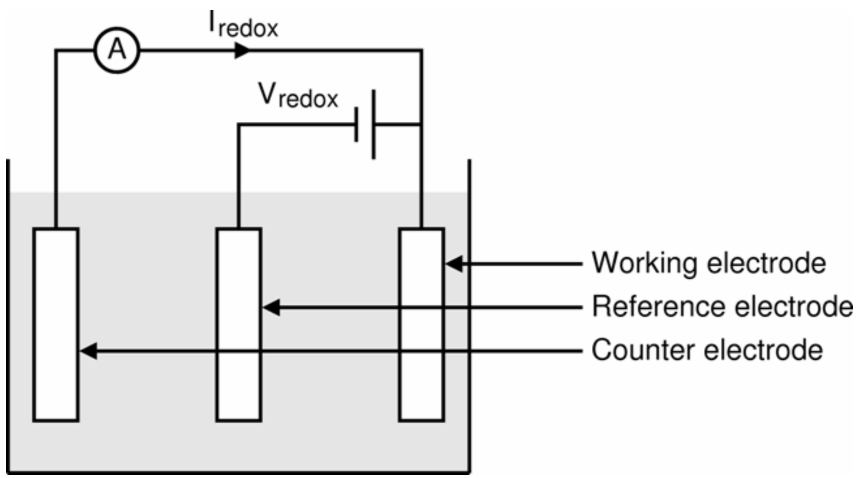

Neurochemical Interface: Circuit Design

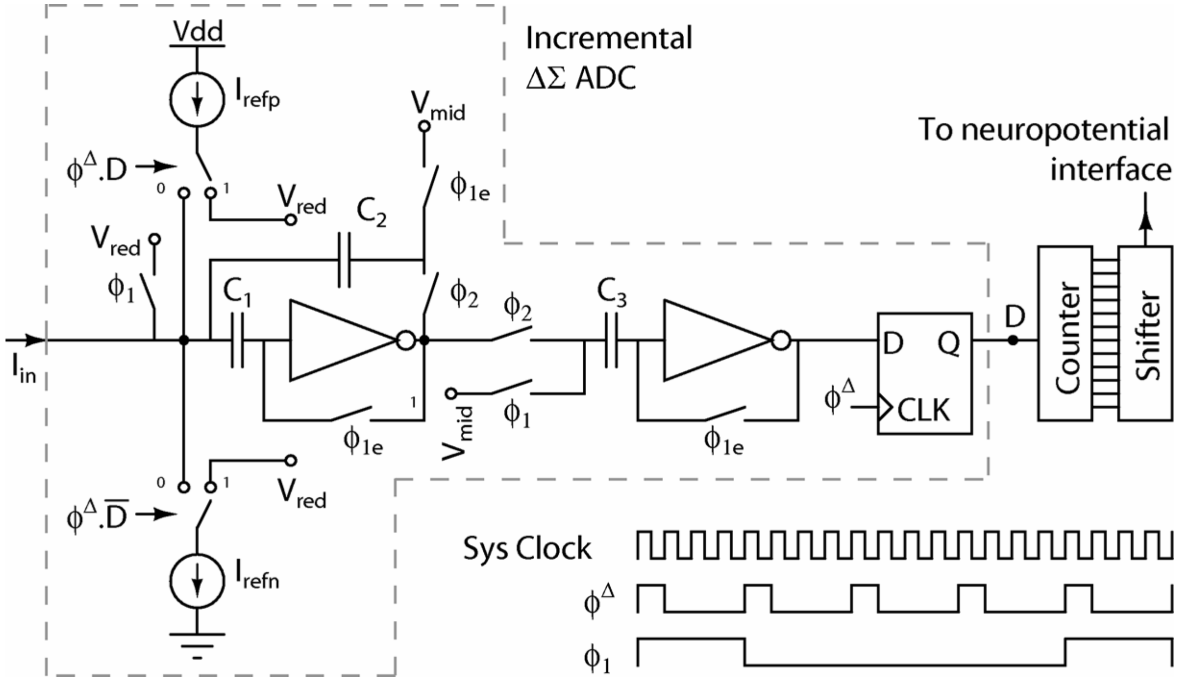

– Current-mode incremental ADC (resetable delta-sigma modulator)

– Duty cycle modulation in DAC delta-sigma feedback implements:

- *programmable digital amplification* G *(at duty cycle 1/*G*);*
- *avoids current amplification, yet accommodates a wide range of input currents, and lowers input current noise.*

Murari et al., BioCAS'2004

VLSI Potentiostat Array for Electrochemical Sensing

Murari, Stanacevic, Cauwenberghs, and Thakor (BioCAS'2004)

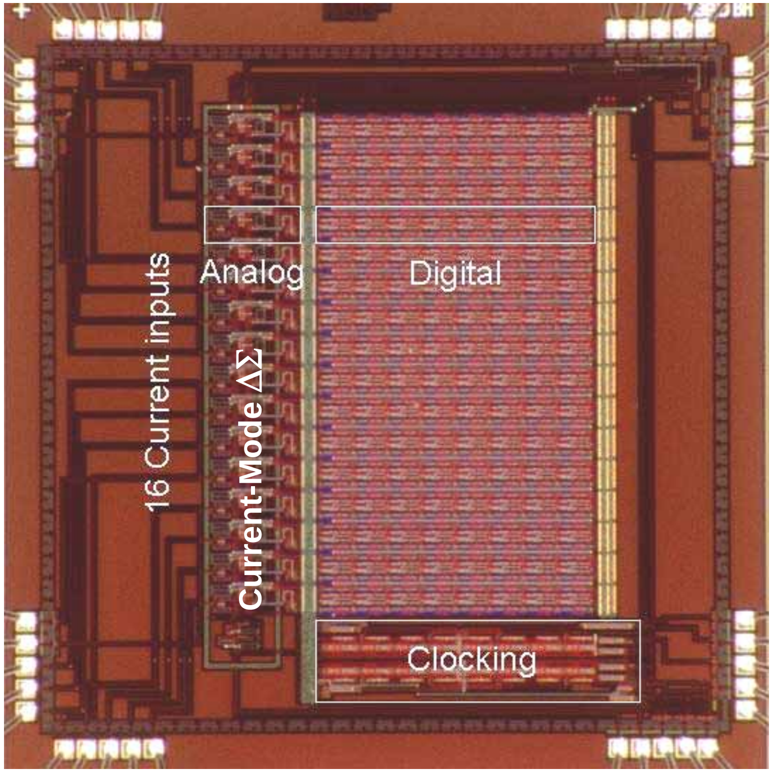

- Distributed neurotransmitter sensing
- Accurate current measurement
  - *6 orders of magnitude range*
  - *1 pA sensitivity*
- Low power
  - *300 μW at 3.3V supply and 1MHz clock*
- Compact
  - *3mm x 3mm in 0.5μm CMOS*

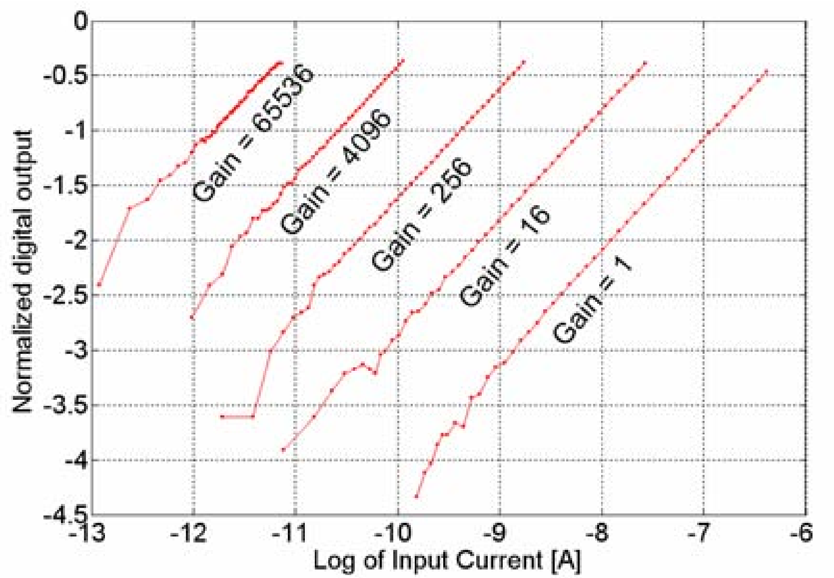

Distributed Sensing of Dopamine Activity

Murari, Stanacevic, Cauwenberghs, and Thakor (EMBS'2004)

Electrochemical detection

Carbon-probe redox current

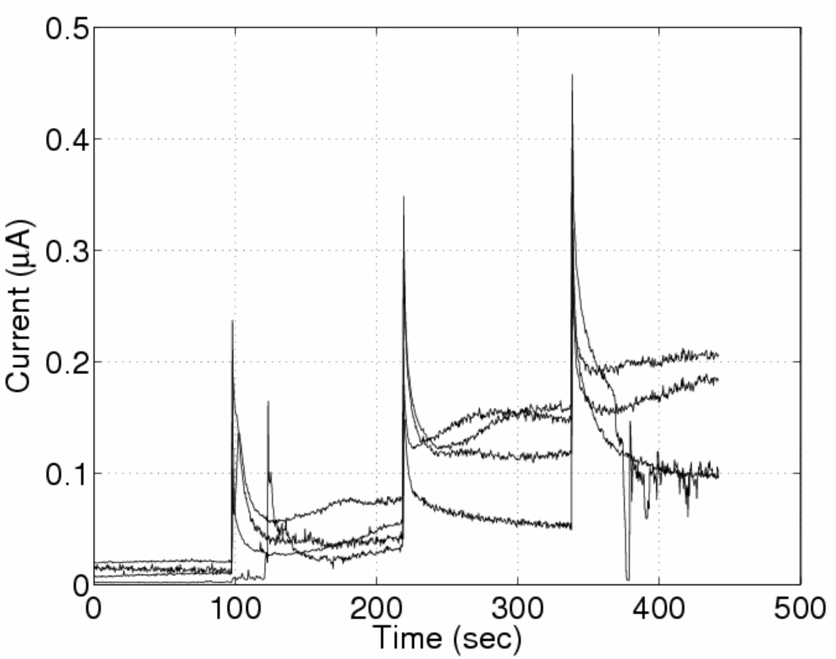

"In vitro" Dopamine monitoring by the chip using micro-fabricated electrode array as working electrode.

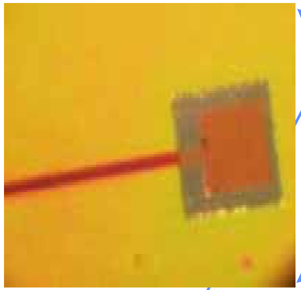

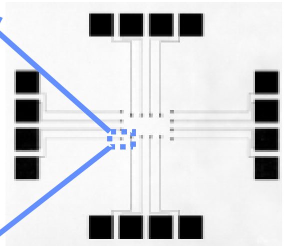

Carbon electrodes for Dopamine sensing
(Murari, Rege, Paul, and Thakor, 2002)

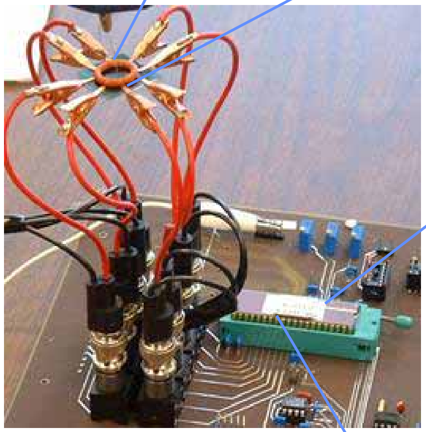

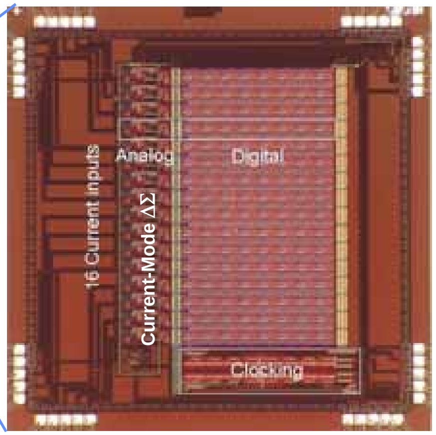

VLSI potentiostat array for distributed electrochemical sensing
(*Murari, Stanacevic, Cauwenberghs, and Thakor, 2004*)

Implantable Wireless Telemetry

- **Transcutaneous wires limit the application of implantable sensing/actuation technology to neural prostheses**
  - Risk of infection
    - *Opening through the skin reduces the body's natural defense against invading microorganisms*
  - Limited mobility
    - *Tethered to power source and data logging instrumentation*

- **Wireless technology is widely available, however:**
  - Frequency range of radio transmission is limited by the body's absorption spectra and safety considerations
    - *Magnetic (inductive) coupling at low frequency, ~1-4 MHz*
    - *Very low transmitted power requires efficient low-power design*

Sauer, Stanacevic, Cauwenberghs, and Thakor, 2005

Implantable Wireless Telemetry

Implantable probe with electrodes, VLSI sensor/actuation processor and power harvesting telemetry chip.

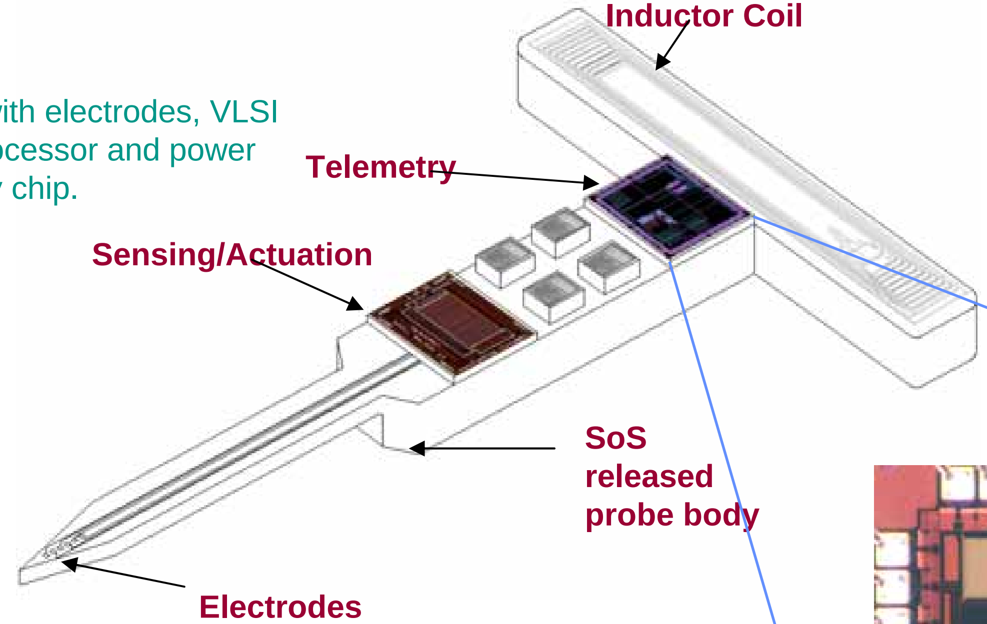

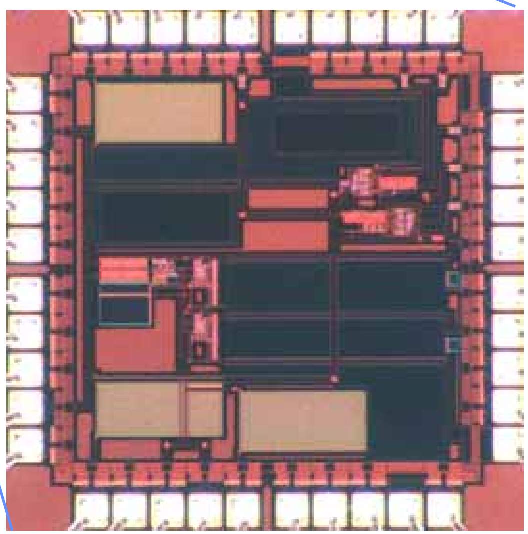

Telemetry chip (1.5mm X 1.5mm)

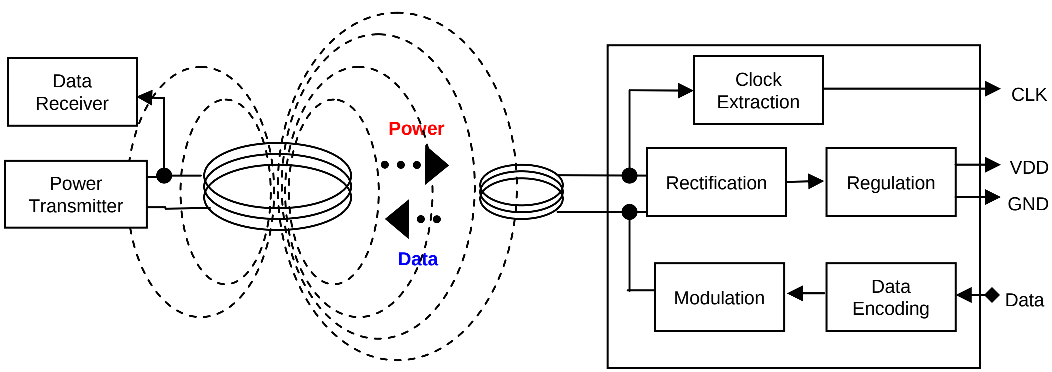

Power delivery and data transmission over the same inductive link

Sauer, Stanacevic, Cauwenberghs, and Thakor, 2005

Signal Extraction

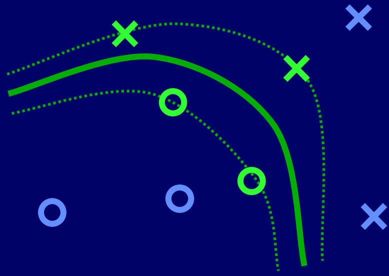

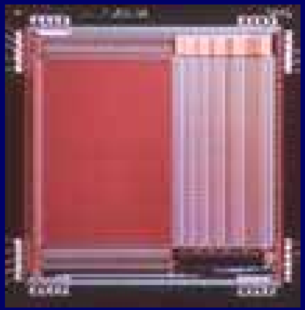

Neuromorphic Systems Engineering

Independent Component Analysis

Adaptive Pattern Recognition

Independent Component Analysis in aVLSI

Solving the Cocktail Party Problem in Real Time

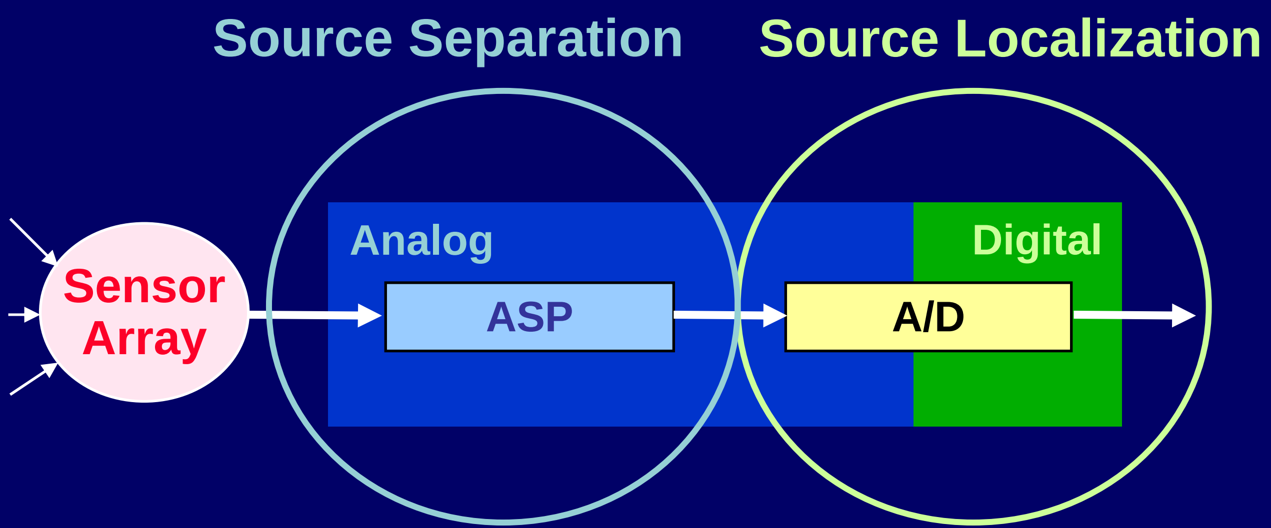

Micropower super-resolution acoustic localization (*ESSCIRC'2003*)

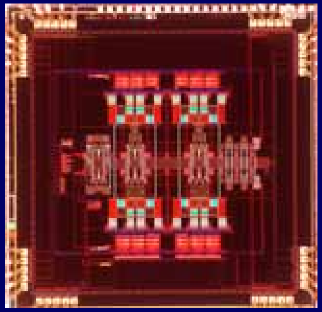

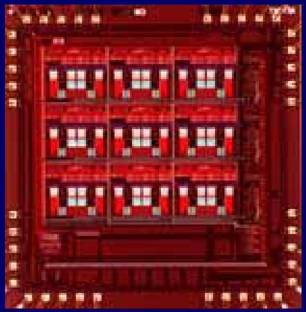

Micropower independent component analysis (*ISCAS'2004*)

Independent Component Analysis

- The task of *blind source separation* (BSS) is to separate and recover independent sources from (instantaneously) mixed sensor observations, where both the sources and mixing matrix are unknown.

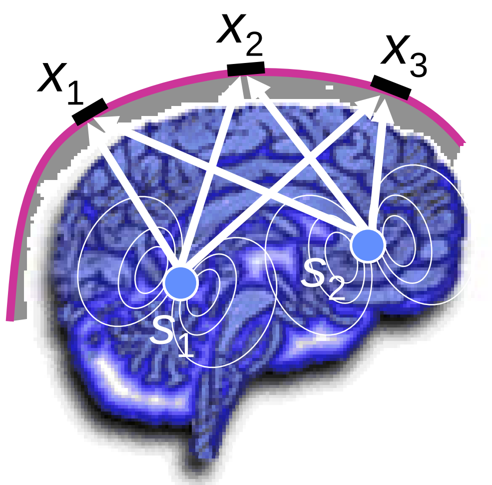

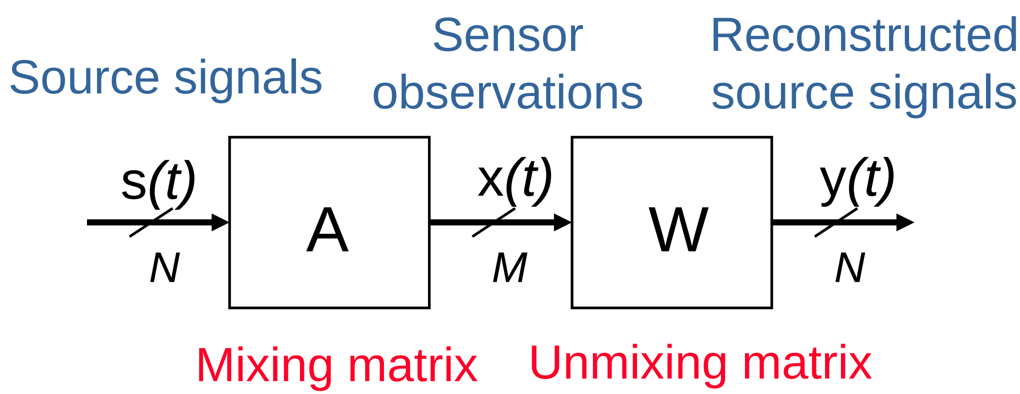

- *Independent component analysis* (ICA) minimizes higher-order statistical dependencies between reconstructed signals to estimate the unmixing matrix.
- Columns of the unmixing matrix yield the spatial profiles for each of the estimated sources of brain activities, projected onto the *scalp map* (sensor locations). *Inverse methods* yield estimates for the location of the centers of each of the dipole sources.

EEG Independent Component Analysis

Swartz Center for Computational Neuroscience, UCSD

http://sccn.ucsd.edu/

- ICA on EEG array data identifies and localizes sources of brain activity.
- ICA can also be used to identify and remove unwanted biopotential signals and other artifacts.
  - *EMG muscle activity*
  - *60Hz line noise*

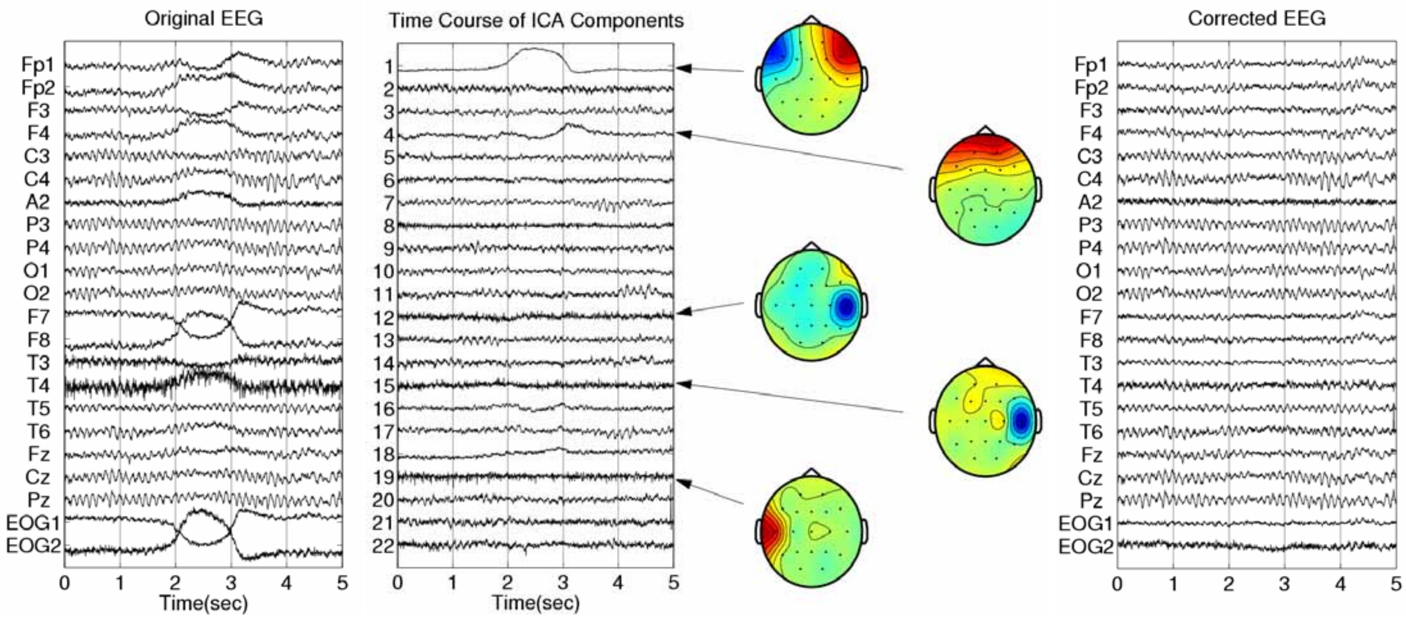

Left: 5 seconds of EEG containing eye movement artifacts. Center: Time courses and scalp maps of 5 independent component processes, extracted from the data by decomposing 3 minutes of 31-channel EEG data from the same session and then applied to the same 5-s data epoch. The scalp maps show the projections of lateral eye movement and eye blink (top 2) and temporal muscle artifacts (bottom 3) to the scalp signals. Right: The same 5 s of data with the five mapped component processes removed from the data [Jung et al., 2000].

Mixed-Signal VLSI Independent Component Analyzer

real-time, micropower blind source separation

Celik, Stanacevic and Cauwenberghs (ISCAS'2004)

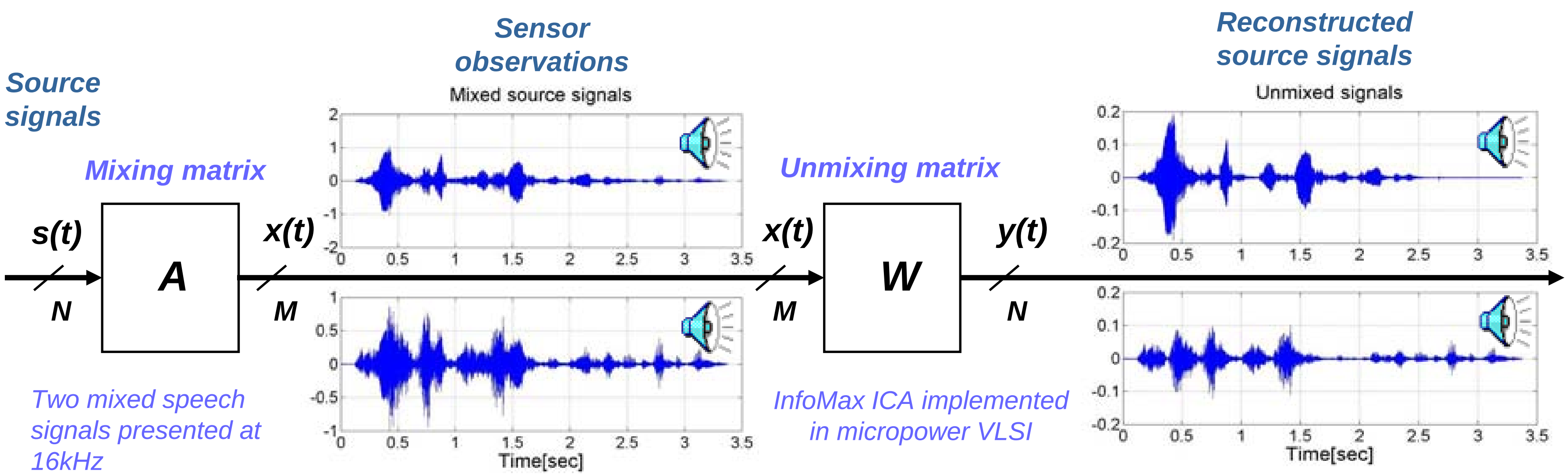

30dB separation observed

- *8-b resolution*
- *16 kHz sampling*
- *180 μW power*
- *3mm x 3mm in 0.5μm 3M2P CMOS*

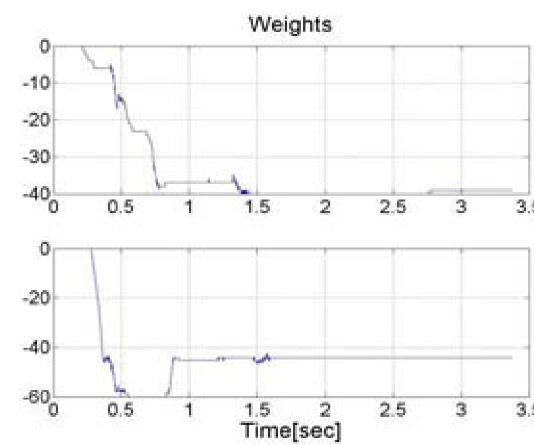

Gradient Flow Independent Component Analysis

integrated acoustic source separation and localization

Celik, Stanacevic and Cauwenberghs (NIPS'2005)

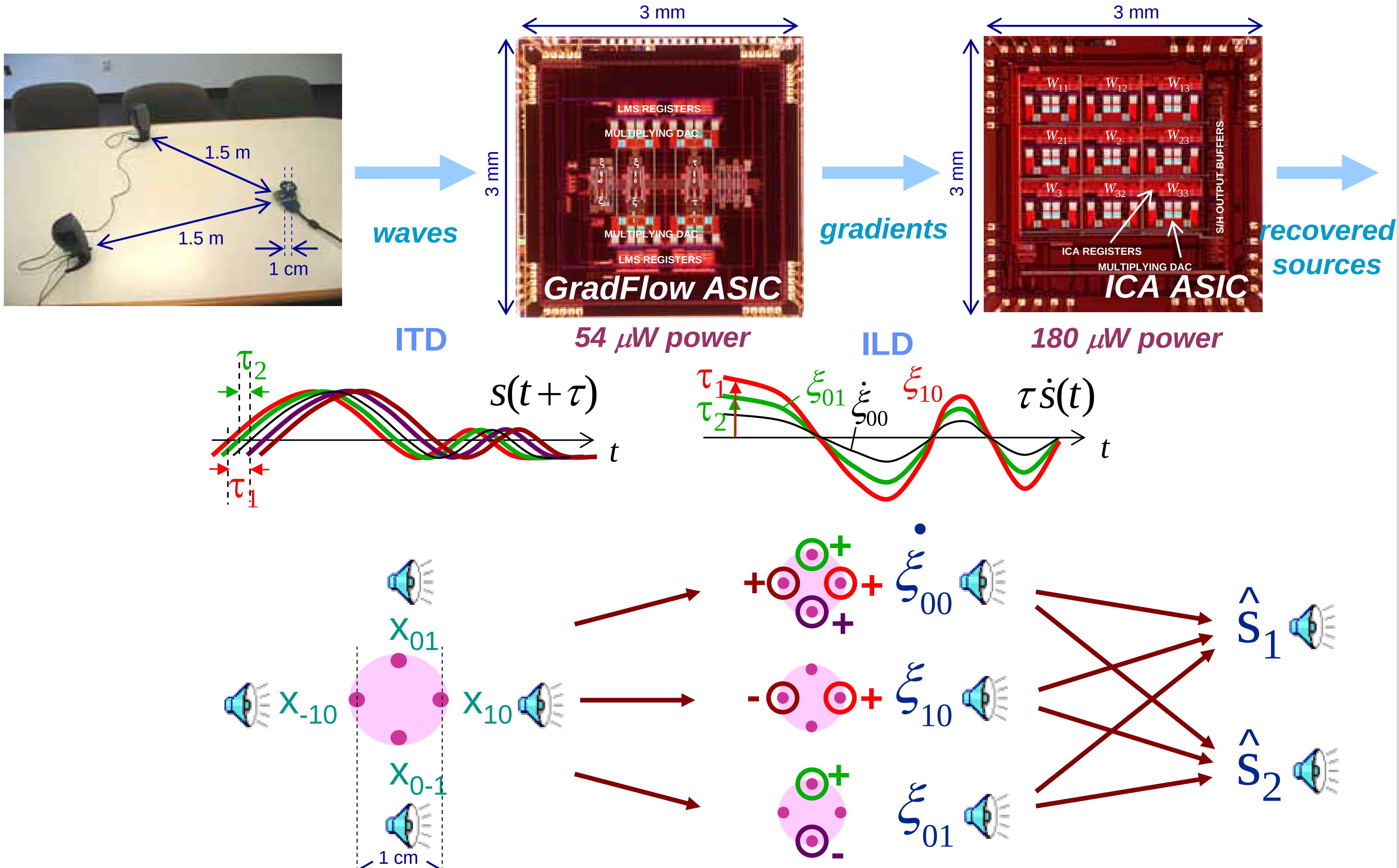

Support Vector Machine (SVM) Adaptive Pattern Recognition

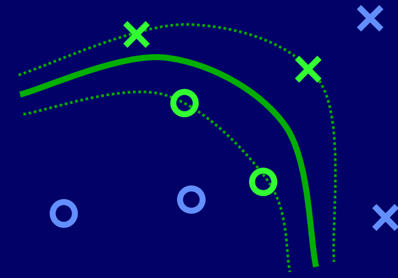

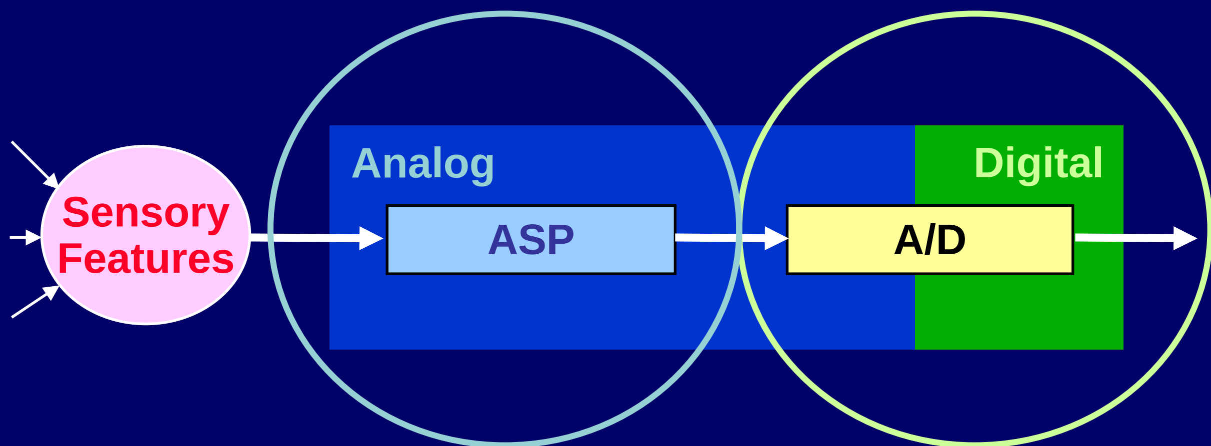

Large-Margin Kernel Regression

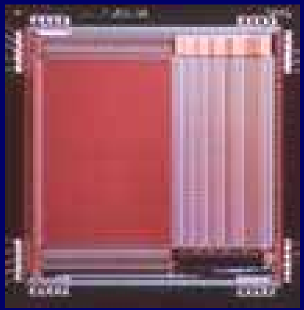

Class Identification

Kerneltron:
massively parallel
support vector
"machine" in silicon
(*ESSCIRC'2002*)

Trainable Modular Vision Systems: The SVM Approach

Papageorgiou, Oren, Osuna and Poggio, 1998

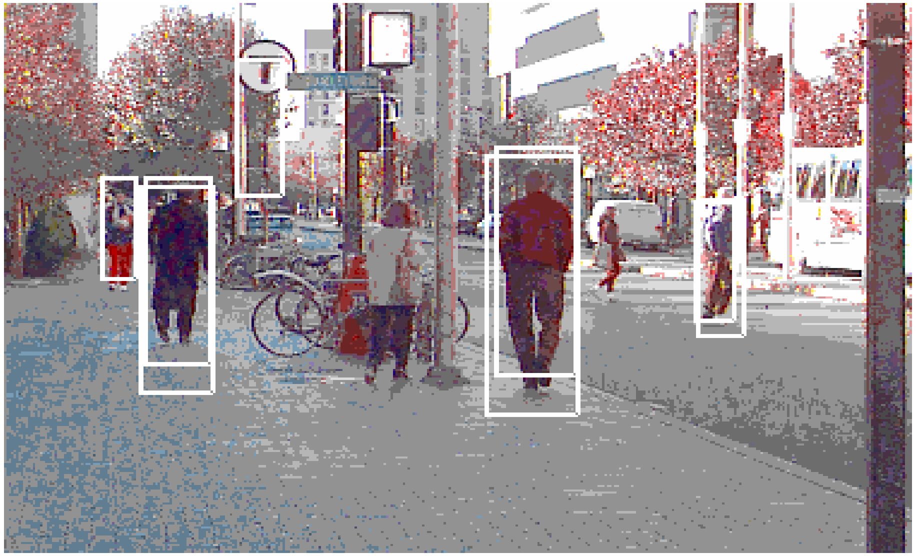

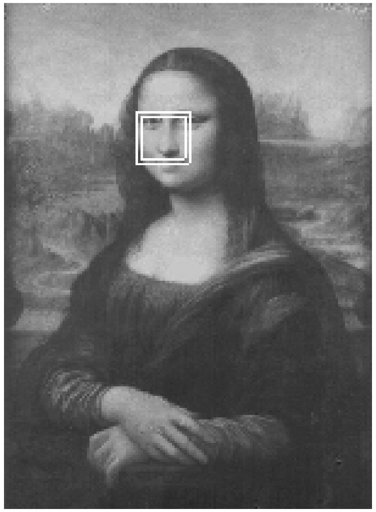

Support vector machine (SVM) classification for pedestrian and face object detection

– Strong mathematical foundations in *Statistical Learning Theory* (Vapnik, 1995)

– The training process selects a small fraction of prototype *support vectors* from the data set, located at the *margin* on both sides of the classification boundary (e.g., barely faces vs. barely non-faces)

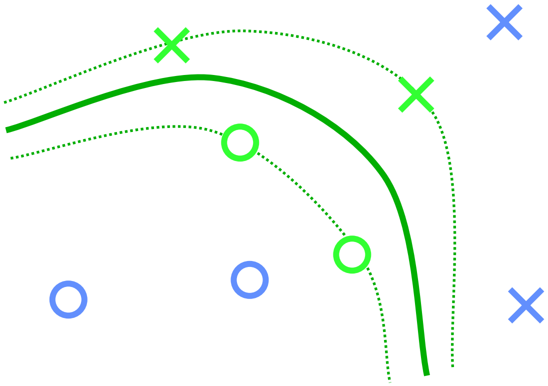

Trainable Modular Vision Systems: The SVM Approach

Papageorgiou, Oren, Osuna and Poggio, 1998

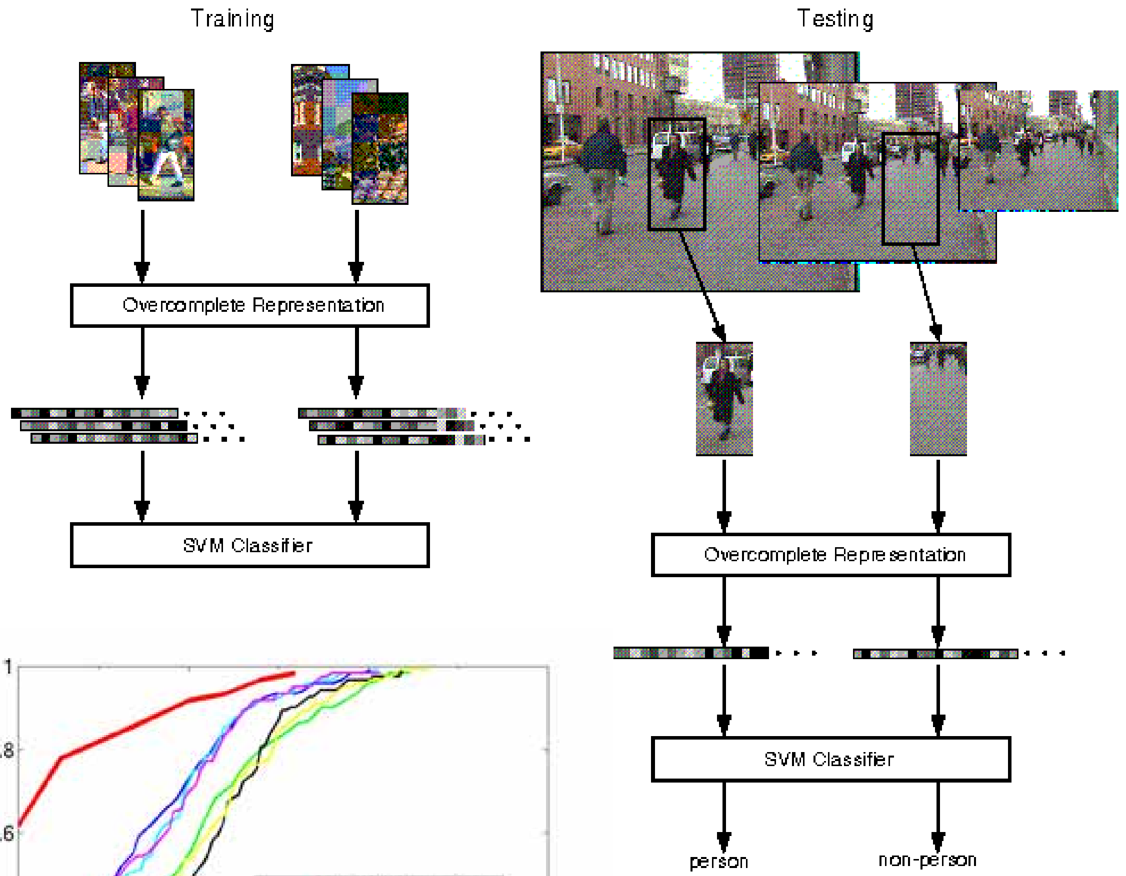

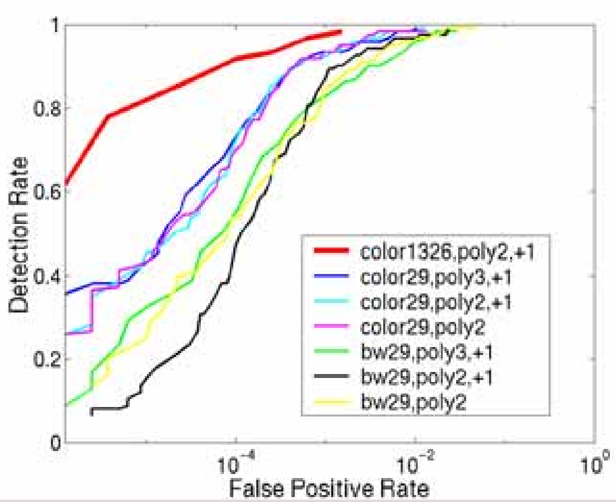

ROC curve for various image representations and dimensions

- The number of support vectors, in relation to the number of training samples and the vector dimension, determine the generalization performance

- Both training and run-time performance are severely limited by the computational complexity of evaluating kernel functions

Kerneltron: Adiabatic Support Vector “Machine”

Karakiewicz, Genov, and Cauwenberghs, VLSI’2006; CICC’2007

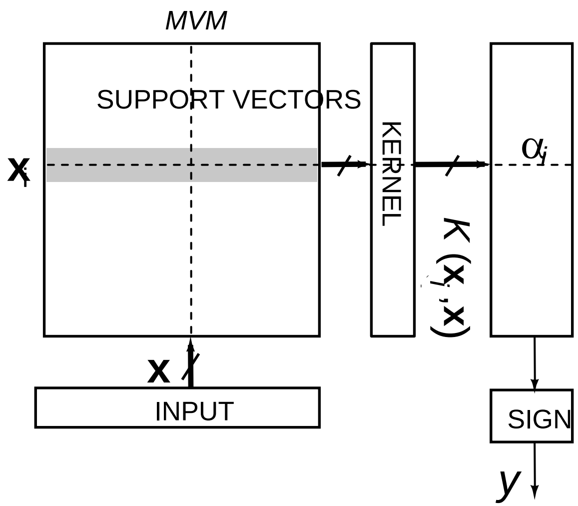

$$y = \mathrm{sign}\Big(\sum_{i\in S} \alpha_i y_i K(\mathbf{x}_i,\mathbf{x}) + b\Big)$$

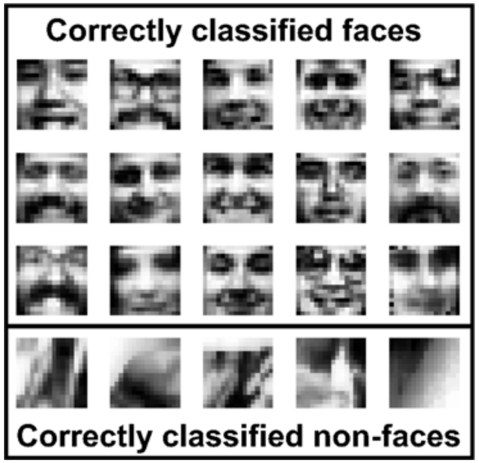

Classification results on MIT CBCL face detection data

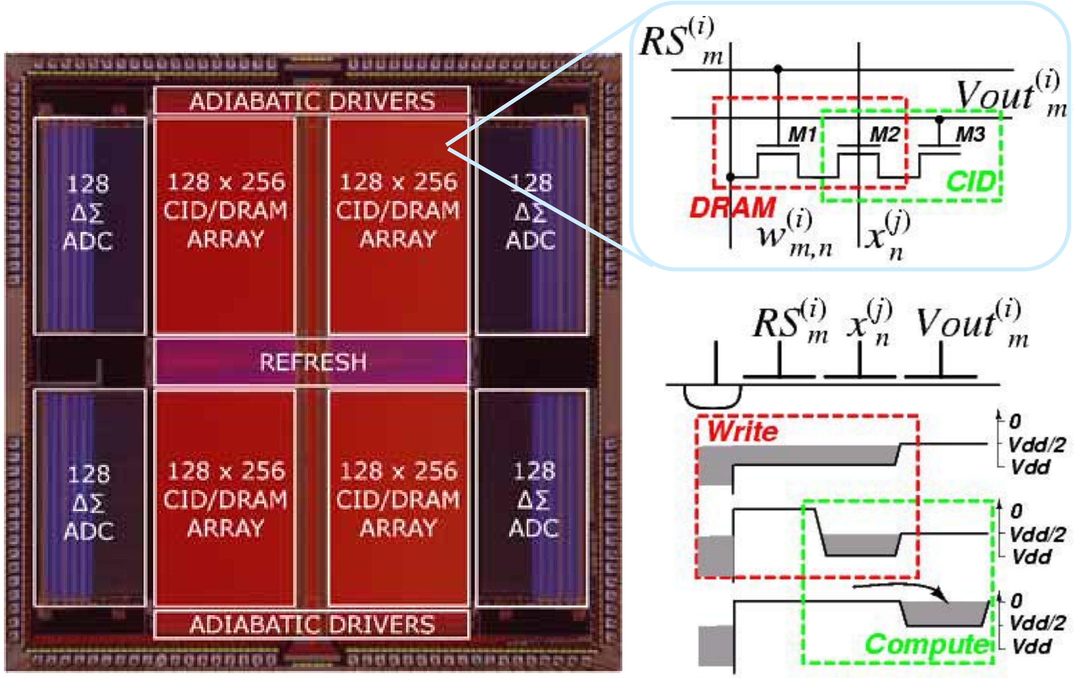

- ***1.2 TMACS / mW***
  - *adiabatic resonant clocking conserves charge energy*
  - *energy efficiency on par with human brain (10^{15} SynOP/S at 15W)*

Resonant Charge Energy Recovery

Karakiewicz, Genov, and Cauwenberghs, IEEE JSSC, 2007

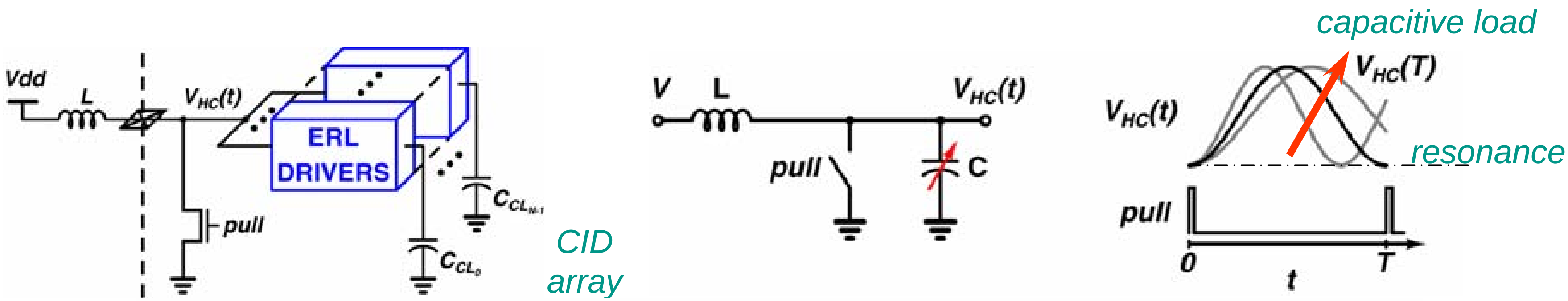

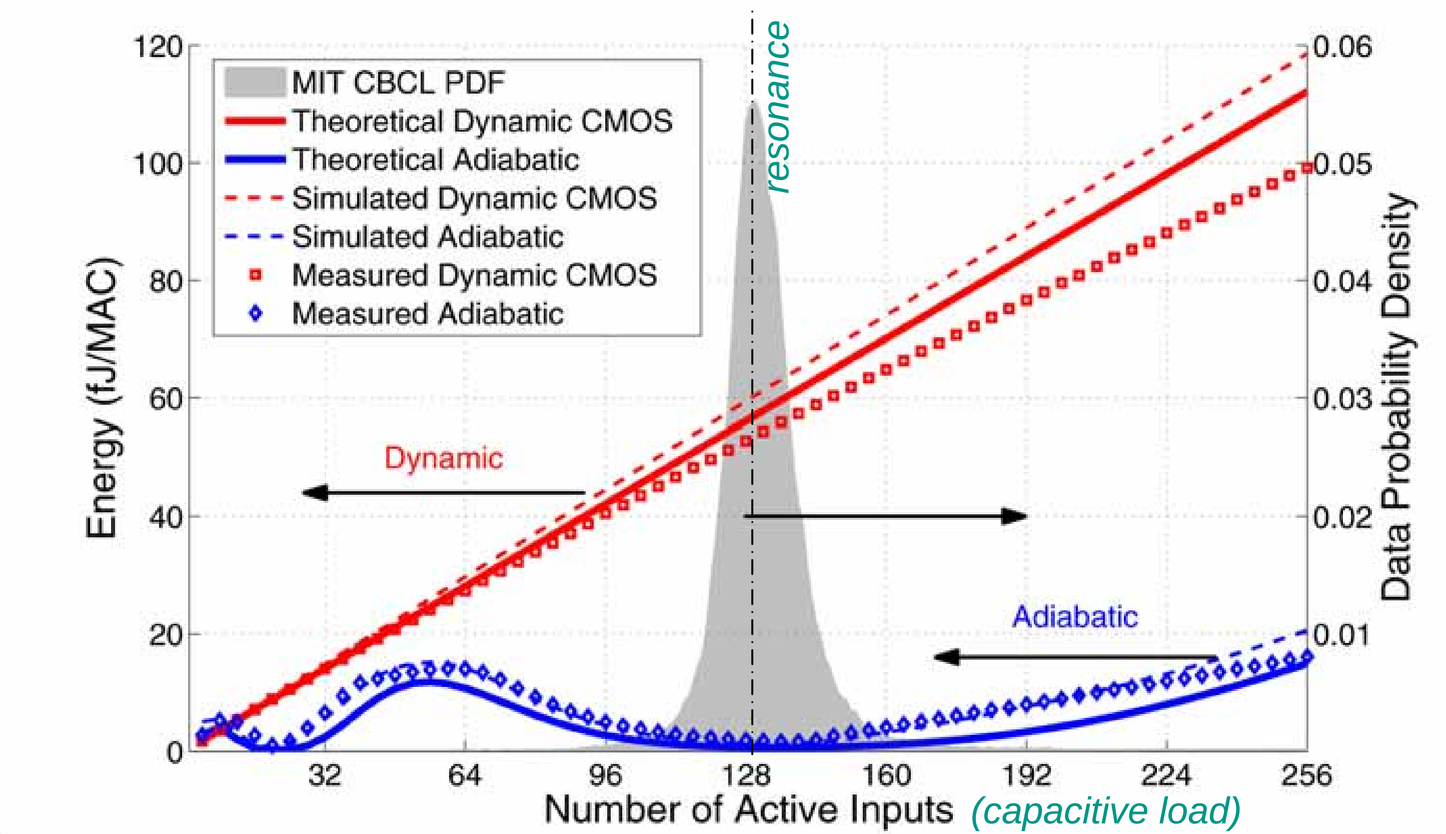

*Gini*SVM/FDKM Processor for Sequence Detection

Chakrabartty and Cauwenberghs (NIPS'2004)

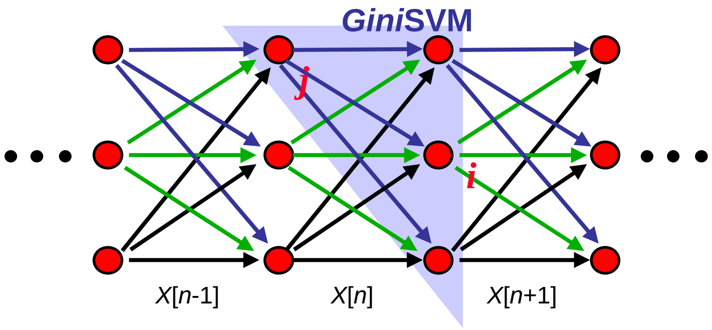

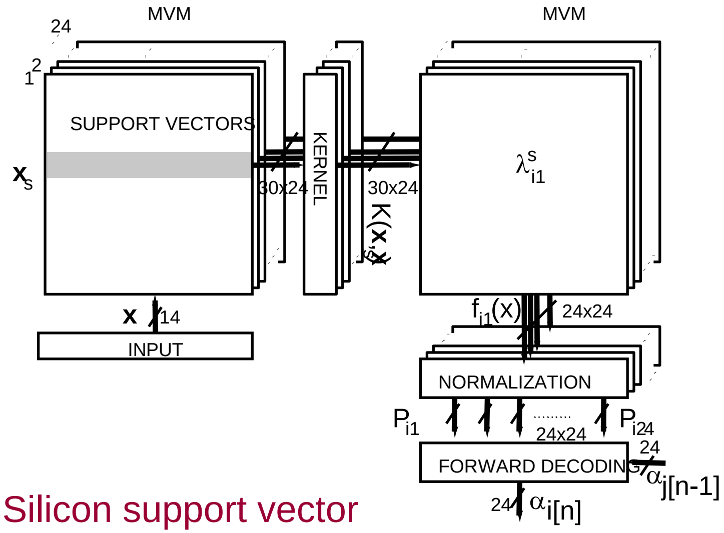

Silicon support vector machine (SVM) and forward decoding kernel machine (FDKM)

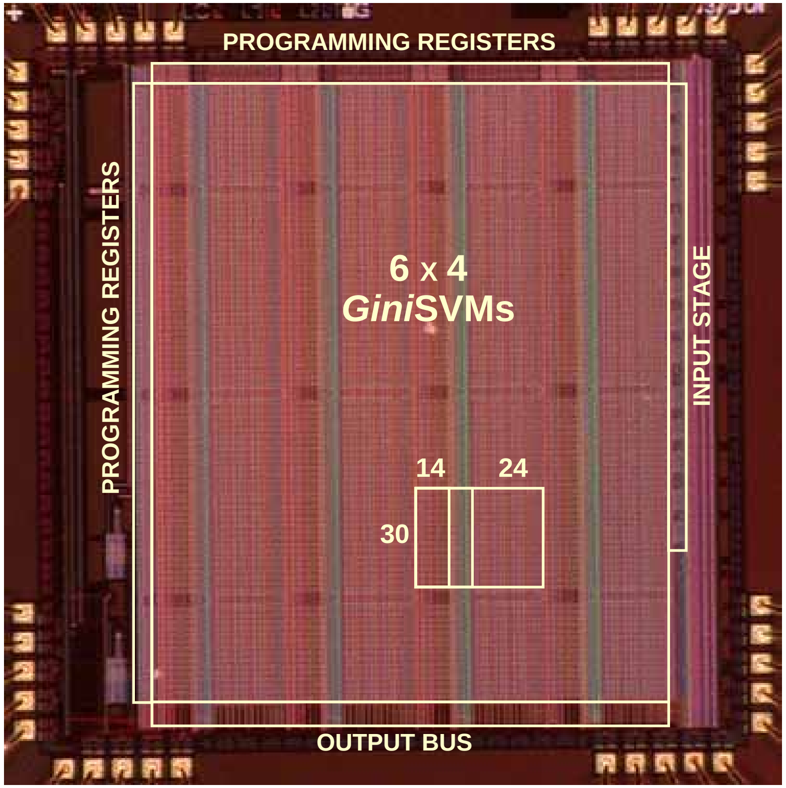

- ***Sub-Microwatt Power***
- *Subthreshold translinear MOS circuits*
- *Programmable with floating-gate non-volatile analog storage*

Integrated Systems Neuroscience/Bioengineering